Roles of Retinoic Acid Signaling in Shaping the Neuronal Architecture of the Developing Amphioxus Nervous System

Elisabeth Zieger, Simona Candiani, Greta Garbarino, Jenifer C. Croce, Michael Schubert

Roles of retinoic acid signaling in shaping the neuronal architecture of the developing amphioxus nervous system

Elisabeth Zieger[1], Simona Candiani[2], Greta Garbarino[2], Jenifer C. Croce[1], Michael Schubert[1,*]

[1]Sorbonne Universités, UPMC Université Paris 06, CNRS, Laboratoire de Biologie du Développement de Villefranche-sur-Mer, Observatoire Océanologique de Villefranche-sur-Mer, 181 Chemin du Lazaret, 06230 Villefranche-sur-Mer, France.

[2]Dipartimento di Scienze della Terra, dell'Ambiente e della Vita (DISTAV), Università di Genova, Viale Benedetto XV, 5, 16132 Genoa, GE, Italy.

*Correspondence to: Michael.Schubert@obs-vlfr.fr

Abstract

The morphogen retinoic acid (RA) patterns vertebrate nervous systems and drives neurogenesis, but how these functions evolved remains elusive. Here, we show that RA signaling plays stage- and tissue-specific roles during the formation of neural cell populations with serotonin, dopamine, and GABA neurotransmitter phenotypes in amphioxus, a proxy for the ancestral chordate. Our data suggest that RA signaling restricts the specification of dopamine-containing cells in the ectoderm and of GABA neurons in the neural tube, probably by regulating *Hox1* and *Hox3* gene expression respectively. The two *Hox* genes thus appear to serve distinct functions rather than to participate in a combinatorial *Hox* code. We were further able to correlate the RA signaling-dependent mispatterning of hindbrain GABA neurons with concomitant motor impairments. Taken together, these data provide new insights into how RA signaling and *Hox* genes contribute to nervous system as well as to motor control development in amphioxus and hence shed light on the evolution of these functions within vertebrates.

Keywords: cephalochordate, serotonin (5-HT), dopamine (DA), γ-aminobutyric acid (GABA), neurotransmitter systems, neuronal specification and differentiation, *Hox* genes, locomotory control

Introduction

Retinoic acid (RA) is a morphogen that, upon entering the nucleus, regulates transcription of target genes by binding to DNA-associated heterodimers of two nuclear hormone receptors, the retinoic acid receptor (RAR) and the retinoid X receptor (RXR) [1, 2]. In vertebrates, RA signaling has been shown to contribute to patterning of the developing nervous system and to controlling the timing of neural progenitor differentiation, by modulating the expression of homeobox genes and other transcription factors [3–6]. RA signaling has further been implicated in the specification of different neural identities and neurotransmitter phenotypes. For instance, RA signaling represses serotonergic (5-hydroxytryptamine, 5-HT) fates in the ventral spinal cord [7, 8], while promoting the dopaminergic (DA) differentiation of neural precursors in the substantia nigra [9, 10] and the γ-aminobutyric acid (GABA) differentiation of striatal projection neurons and interneurons in the basal ganglia [11]. Chiefly through pharmacological treatments, RA has been shown to also affect developmental processes in various non-vertebrate taxa, including cnidarians, gastropod mollusks, and non-vertebrate chordates [12–19]. Yet, little is known about the precise roles of RA signaling during the formation of neural cell populations in non-vertebrate animals [20].

As slow evolving sister group of all other chordates (i.e. tunicates plus vertebrates) [21–23], the cephalochordate amphioxus represents an important model organism for studying the evolution of both neural development and RA signaling functions [20, 24–26]. For instance, amphioxus is characterized by a nervous system with a vertebrate-like organization, but with a limited number of only about 20,000 neurons [27, 28]. The adult central nervous system (CNS) of amphioxus consists of a dorsal hollow nerve cord that shows no external structuring, apart from a caudal ampulla and serially repeated dorsal nerves, which lack ganglia [28]. Nonetheless, regions with distinct internal anatomy and cell type composition can be distinguished and, during pre-metamorphic stages, a transient anterior thickening is present that is generally referred to as cerebral vesicle (CV) or brain [28, 29]. This larval CV opens to the exterior via a dorsal neuropore and contains an anterior frontal eye, which is thought to be homologous to the paired eyes of vertebrates, as well as a posterior

ventral cluster of secretory infundibular cells [28, 30–32]. Developmental gene expression studies together with detailed neuroanatomical analyses have revealed that the regionalization of the larval amphioxus CNS largely corresponds to that of developing vertebrates and comparisons between the two can thus provide important insights into the evolution of neural development in chordates [25, 33, 34].

Contrary to vertebrates, however, the peripheral nervous system (PNS) of amphioxus develops from a ventral neuroectodermal precursor field. Here, migratory neural progenitors become specified that express different sets of neural genes [35]. Importantly, several of these genes are related to marker genes of vertebrate cranial placodes [35–37]. Once the migratory progenitors reach the flanks of the amphioxus larva, they give rise to different types of epidermal sensory neurons (ESNs), which project an axon into the neural tube and may exhibit modified spine-like cilia or a collar of branched microvilli [28, 38, 39]. Furthermore, peripheral plexuses that receive synaptic inputs from intrinsic and extrinsic neurons, such as the oral nerve plexus, have been described [28, 40].

Throughout the developing amphioxus nervous system, the distribution of progenitor populations expressing different neural marker genes has been shown to depend on RA signaling [36, 41]. Given that cephalochordates have not experienced the whole genome duplications of vertebrates [42–44], amphioxus possesses only a single retinoic acid receptor (*rar*) and a single retinoid X receptor (*rxr*) gene, while vertebrate genomes generally encode three *rar* (*rar*α, *rar*β, and *rar*γ) and three *rxr* (*rxr*α, *rxr*β, and *rxr*γ) genes [20]. Nonetheless, the RA signaling pathway of amphioxus appears to function in a similar manner as in vertebrates, through a posterior-high RA gradient that controls the collinear expression of *Hox* genes and thus axial patterning of the embryo [16, 36, 41, 45, 46]. Together, these findings support the notion that RA signaling plays comparable roles during amphioxus and vertebrate nervous system development [20, 47], even though the precise functions of RA signaling during establishment of distinct neural cell populations remain to be assessed.

Several neurotransmitter systems have already been identified in the larval amphioxus nervous system. 5-HT neurons, for instance, appear to be restricted to the anterior-most brain region, while expression of enzymes involved in the synthesis

of DA and GABA have been detected, respectively, in the caudal CV and along the hindbrain-like portion of the neural tube [27, 48, 49]. Amphioxus adults exhibit corresponding populations of 5-HT- and DA-containing neurons within their anterior neural tube [50], whereas GABAergic neurons are more widely spread throughout their entire CNS and PNS [51]. This study traces the distribution of 5-HT, DA, and GABA cells from early embryonic through larval development in the European amphioxus, *Branchiostoma lanceolatum*, through both gene expression and immunohistochemical approaches. The obtained results expand the existing data, by providing detailed new insights into the neurochemical architecture of the developing amphioxus nervous system. Using pharmacological treatments, we further explore how RA signaling affects the formation of different neural cell populations within both the CNS and PNS of amphioxus larvae. These findings highlight the stage and tissue specificity of RA signaling activities. Notably, at least some of the observed RA signaling functions might be mediated by individual *Hox* genes that appear to play distinct roles instead of acting in a combinatorial fashion. Finally, we also identify an important requirement of RA signaling for the acquisition of motor control in amphioxus larvae, which we propose to be linked to the RA-dependent patterning of hindbrain GABA neurons. Taken together, our results complement research in tunicates and vertebrates, enabling us to formulate novel hypotheses regarding the evolution of RA signaling and *Hox* gene functions during chordate nervous system development.

Results

Retinoic acid signaling does not affect the formation of serotonergic neurons in the anterior cerebral vesicle of amphioxus

Using an antibody directed against 5-HT, we characterized the distribution of 5-HT immunoreactivity (-ir) in embryos and larvae of the European amphioxus (*B. lanceolatum*). 5-HT-ir first became discernable in feeding larvae at about 36 hours post fertilization (hpf) (Fig. 1a,a'). At this stage as well as at later stages, a single group of three to five neurons exhibiting 5-HT-ir was present in the anterior ventral part of the CV, in the area of the frontal eye complex (Fig. 1b,b'-d,d'). Dorsally these neurons were in contact with the lumen of the neuropore and ventrally their neurites projected in both anterior and posterior direction through the rostral nerves (Fig. 1c,c',d,d'). The anterior-most 5-HT-ir neurons were closely associated with the pigment spot of the amphioxus frontal eye (Fig. 1c''). Importantly, the 5-HT-ir endocrine cells in the ileo-colon ring of the larval gut, which have been described for the Florida amphioxus (*B. floridae*) [48], were not detectable in *B. lanceolatum* larvae.

To assess, whether RA signaling influences the formation of 5-HT-ir neurons, we exposed *B. lanceolatum* embryos at either 6 hpf (late blastula stage) or 24 hpf (neurula stage) to the RAR antagonist BMS493 or to exogenous all-*trans* RA. None of these treatments affected the presence and distribution of 5-HT-ir neurons in the anterior CV of amphioxus larvae in a statistically significant manner (Fig. 1e-g,f',g'). The average number of 5-HT-ir cells ranged from a minimum of 3.4 cells in embryos treated with RA at 6 hpf (σ=1.5; n=5) to a maximum of 4.6 cells in embryos treated with RA at 24 hpf (σ=1.4; n=7), with an average of 3.8 cells in controls (σ=0.75; n=5). Thus, RA signaling is dispensable for the development of 5-HT neurons in the amphioxus CV.

Retinoic acid signaling influences dopaminergic cell development in amphioxus in a stage- and tissue-dependent manner

As is the case for 5-HT-ir, DA-ir first became detectable in *B. lanceolatum* larvae at 36 hpf, in a cluster of thickened ectodermal cells (Fig. 2a,a') that have previously been described as the right papilla [52]. Accordingly, this DA-ir cell cluster was located on the right side of the amphioxus larvae, in the ectoderm ventral to the club-shaped gland (an enigmatic amphioxus-specific organ producing mucus) and just posterior to the endostyle (the amphioxus homolog of the vertebrate thyroid gland), but anterior to the first gill slit (Fig. 2c,c',d,d',e). The average number of cells in the DA-ir cell cluster increased from 7 at 36 hpf (n=17, σ=2.29) (Fig. 2a,a'), to 13 at both 60 (n=14, σ=1.72) and 108 hpf (n=11, σ=1.23) (Fig. 2b,b'-d,d'). In general, the DA-ir cells were arranged in a circular or semi-circular manner and counterstaining with an antibody against acetylated tubulin revealed that they did not possess neurites. Instead, an array of small acetylated tubulin-ir structures, which might correspond either to basal bodies of cilia or to severely truncated neurites, was closely associated with the DA-ir cluster (Fig. 2c'').

We next investigated how altering RA signaling levels during amphioxus development (at 6, 12, 24, 36, and 48 hpf) affected DA-ir cells in larvae at 60 hpf. Treatments with the RAR antagonist BMS493 resulted in a gain of additional DA-ir cells, with earlier treatments inducing a stronger effect than later treatments (Fig. 2f-j). Some larvae treated with BMS493 at 6 hpf (late blastula stage) or 12 hpf (gastrula stage) thus had more than 20 DA-ir cells (Fig. 2f,h,i), while no effect was observed in animals that were treated at larval stages, such as at 36 or 48 hpf (Fig. 2f,g,k,l). Interestingly, following BMS493 treatments, DA-ir cells were added only in posterior direction, so that the DA-ir cell cluster was expanded posteriorly, in the most extreme cases to levels caudal to the first gill slit (Fig. 2h). Conversely, early RA treatment, at 6 hpf, completely abolished DA-ir (Fig. 2f,g,h'). Later RA treatments at 12 hpf or 24 hpf (neurula stage), on the other hand, only led to a partial loss of DA-ir cells, with most larvae possessing four to five DA-ir cells instead of 13 as in controls (Fig. 2f,g,i',j'). Finally, no effect on the presence of DA-ir cells was observed, if RA treatments began at even later larval stages (36 or 48 hpf) (Fig. 2f,k',l'). Together,

these results suggest that, during early development, RA signaling is critical for restricting the formation of DA-ir cells to anterior ectoderm.

Of note, DA-ir was absent from the developing *B. lanceolatum* neural tube, although this neurotransmitter is widely distributed throughout the CNS of most animals [53–55] and has been detected in the anterior nerve cord of *B. lanceolatum* adults [50]. Moreover, it was shown that tyrosine hydroxylase (TH), an enzyme involved in DA synthesis, is expressed in the CV of *B. floridae* larvae [56]. To corroborate our findings, we thus analyzed TH-ir in *B. lanceolatum* larvae. At 36 hpf, TH-ir was inconspicuous in cells corresponding to the right papilla/DA-ir cell cluster (Fig. 3a,a'), but it became clearly visible in this structure between 48 and 60 hpf (compare Fig. 2c',c'' and Fig. 3c',c''). In the latter stages, TH-ir was further present in the posterior CV (Fig. 3b,c,b',c'), matching the pattern reported for *B. floridae* larvae [56]. However, late *B. lanceolatum* larvae exhibited additional TH-ir in two clusters of small, bottleneck-shaped cells within the endostyle, throughout the club-shaped gland, and at the pigment spot of the frontal eye (Fig. 3c,d). Also, at all analyzed stages low levels of TH-ir were observed in the general ectoderm, especially in the tail region (Fig. 3a-d). In *B. floridae*, *TH* expression has not been observed in these peripheral structures [56], but this might be due to very low overall transcription levels of *TH* mRNA in the ectoderm of amphioxus larvae.

In amphioxus larvae that were treated at 6 hpf and fixed at 60 hpf, altered RA signaling levels affected the ectodermal TH-ir cells of the right papilla in the same way as the DA-ir cells of the right papilla. Accordingly, more of them were detected in BMS493-treated larvae, while they were lost in RA-treated larvae (Fig. 3e-g,e'-g'). In contrast, the TH-ir neurons in the posterior CV were consistently disorganized, but not abolished, by early RA treatments, yet unaffected by early BMS493 treatments (Fig. 3e-g). This malformation of TH-ir neurons in the posterior CV following RA treatment is likely due to a general posteriorization of the CNS induced by ectopic RA signaling activity [57]. We hence conclude that, during early amphioxus development, RA signaling is required for patterning the anterior ectoderm by establishing the posterior limit of the DA-ir cell cluster, but not for patterning TH-ir neurons in the CV.

Retinoic acid signaling differentially controls the development of GABAergic neurons in the amphioxus central and peripheral nervous system

GABA-ir already became visible in *B. lanceolatum* larvae at about 30 hpf (Fig. 4a,b), in three segmentally arranged neuronal cell clusters that were separated by 20-25 µm (Fig. 4b). From these GABA-ir neurons, short neurites extended in posterior direction through the neural tube. Each neurite exhibited a thickened ending that elongated towards the posterior end of the neural tube during subsequent development and thus likely corresponds to an axonal growth cone (Fig. 4b,c,c1-c4). At 36 hpf, the first, anterior-most, GABA-ir cell cluster comprised a pair of strongly labeled GABA-ir neurons as well as two to three weakly stained GABA-ir neurons, all of which were located at the posterior limit of the CV (Fig. 4c,c1). In contrast, the second GABA-ir cell cluster typically comprised only a pair of strongly labeled GABA-ir neurons, which were positioned at the level of the boundary between the second and third somite (Fig. 4c,c2). The number of cells in the third GABA-ir cell cluster varied between two and four neurons that were situated at the level of the boundary between the third and the fourth somite (Fig. 4c,c3). Interestingly, 3D projecting confocal image stacks of larvae at 36 hpf further revealed that, just posterior to each of the three initial GABA-ir cell clusters, GABA-ir neurites crossed each other to project along the contra-lateral side of the neural tube (Online Resource 1). Between 48 and 108 hpf, additional GABA-ir cells appeared along the trunk region of the neural tube, in an area posterior to the third GABA-ir cell cluster, but their number and arrangement differed considerably between specimens (Fig. 4d-f).

From 36 hpf, GABA-ir neurons also became visible in the amphioxus ectoderm (Fig. 4c). These neurons were characterized by a single axonal projection into the neural tube as well as by numerous dendritic fibers that extended across the surface of the ectoderm and, at later developmental stages, formed a complex network (Fig. 4d-f,g''). The morphology of these cells suggests that they are primary (type I) ESNs (Fig. 4g,g',g'', arrows) [58]. Between 60 and 108 hpf, another system of interconnected GABA-ir neurons developed in the anterior ectoderm: at the pre-oral pit, around the mouth, and innervating the first gill silt (Fig. 4e-g,g', arrowheads). These neurons did not exhibit any visible connection to the CNS and might thus be part of an independent visceral nervous system (Fig. 4g,g'). Most likely they

contribute to the oral nerve plexus of amphioxus larvae, which is thought to receive sensory information from oral spine cells and to control feeding as well as food rejection responses [37, 40]. Located at the pre-oral pit, the anterior-most cell of this visceral GABA-ir system was a very large neuron with several conspicuous neurites (Fig. 4g', arrowhead pointing downward). One of these neurites innervated a ring of four to six interconnected GABA-ir neurons that were dispersed around the mouth of the larva (Fig. 4g', arrowheads pointing upward). In addition, one or more other neurites passed the mouth ventrally and, posterior to it, joined projections from the GABA-ir ring cells, which crossed the ventral midline from the left to the right side of the larva to innervate the gill slit (Fig. 4g).

We next assessed how manipulation of RA signaling levels during amphioxus development (at 6, 12, and 24 hpf) influences GABA-ir neurons in the CNS (at 36 hpf) and in the PNS (at 60 hpf). In the CNS, early exposure to the RAR antagonist BMS493 resulted in the acquisition of additional GABA-ir cell clusters at more posterior levels of the developing CNS (Fig. 5a-e,a'). Larvae that had been treated at 6 or 12 hpf exhibited on average 4.6 or 4.4 GABA-ir cell clusters, respectively (Fig. 5e). Later BMS493 treatments, at 24 hpf, had no effect on the number of GABA-ir cell clusters (Fig. 5e). Moreover, posterior projections from GABA-ir neurons in the larval neural tube were not noticeably altered by any BMS493 treatment (Fig. 5b-d). In comparison, early RA treatments, carried out at 6 and 12 hpf, led to a partial loss of GABA-ir neurons (Fig. 5a,e,a'-d'). Instead of three, only one GABA-ir cell cluster was thus present in larvae at 36 hpf (Fig. 5e). The position of this single GABA-ir cell cluster, at the posterior limit of the CV, corresponded to that of the anterior-most GABA-ir cell cluster in controls (Fig. 5a,a'), suggesting that early RA treatments selectively act on the development of the two posterior GABA-ir cell clusters. In response to late RA treatments, at 24 hpf, all three GABA-ir cell clusters were formed normally. However, all RA treatments reduced posterior projections from GABA-ir neurons in the larval neural tube, strongly for treatments at 6 hpf and slightly for treatments at 12 and 24 hpf (Fig. 5b'-d'). These findings show that RA signaling influences neurite outgrowth in amphioxus larvae and, during early development, patterns the hindbrain-like portion of the CNS by defining the posterior limit of a territory that gives rise to GABA cluster-containing segments. Of note, the latter

function is comparable to how RA signaling regulates patterning of the anterior ectoderm by restricting DA-ir cell cluster formation.

In the PNS, formation of GABA-ir ESNs was affected differently by changing RA signaling levels than GABA-ir neurons in the CNS. For convenience and visibility, this was documented in amphioxus larvae at 60 hpf (Fig. 6). To assess the distribution of GABA-ir ESNs, larvae were subdivided into three sections of equal size (anterior, middle, and posterior), along their anterior-posterior axis. On average, seven GABA-ir ESNs were present in the anterior part of control larvae (σ=1.4; n=10) and four in the middle part (σ=2.6, n=10) (Fig. 6a,e,a'). In the posterior part, GABA-ir ESNs were mostly absent, although in two of ten animals one GABA-ir neuron was observed. Early BMS493 treatments, at 6 and 12 hpf, led to a significant reduction of GABA-ir ESNs in the anterior part of the amphioxus larvae, resulting in an average of 3.6 (σ=0.8; n=9) and 1.4 (σ=1.5; n=7) GABA-ir cells, respectively (Fig. 6b-e). In contrast, late BMS493 treatments, at 24 hpf, as well as treatments with RA did not significantly affect the number and distribution of GABA-ir ESNs (Fig. 6d,e,b'-d'). RA signaling activity is thus required during early development to promote the GABAergic differentiation of ESNs in the anterior amphioxus PNS.

Finally, altering RA signaling levels influenced the visceral GABA-ir system of amphioxus larvae at 60 hpf in a similar way as both GABA-ir cell clusters in the CNS and DA-ir cells in the ectoderm. While BMS493 treatments had no effect on the presence of the large GABA-ir neuron at the pre-oral pit, they increased the number of GABA-ir cells around the mouth in six of nine animals for treatments at 6 hpf and in five of seven animals for treatments at 12 hpf (Fig. 6a-d; Fig. A1a-d). Notably, most of the additional GABA-ir cells were located ventral to the mouth (Fig. 6b,c; Fig. A1b,c). BMS493 treatments further abolished GABA-ir projections to the gill slits in eight of nine animals for treatments at 6 hpf, in six of seven animals for treatments at 12 hpf, and in three of six animals for treatments at 24 hpf (Fig. 6b-d; Fig. A1b-d). In comparison, early RA treatments abolished all visceral GABA-ir neurons, along with the structures they normally innervate, e.g. the mouth and gill slits (Fig. 6a,a',b'; Fig. A1a,b'). This is consistent with a general loss of anterior structures in amphioxus larvae that were exposed to exogenous RA from early embryogenesis onward [57]. Following later RA treatments, at 12 and 24 hpf, the complex system of visceral

GABA-ir neurons was partially formed. The large GABA-ir neuron located at the pre-oral pit was present in either three of ten or in all animals treated at 12 or 24 hpf, respectively, while GABA-ir neurons projecting in a ring around the mouth were only visible in four of ten animals treated at 24 hpf (Fig. 6c',d'; Fig. A1c',d'). Moreover, GABA-ir neurites extending towards the gill slit were absent in all RA-treated animals (Fig. 6b',c',d'; Fig. A1b',c',d'). In the developing amphioxus PNS, RA signaling thus patterns visceral GABA neurons and regulates the outgrowth of their neurites.

To confirm our results, we investigated the expression of *GAD* mRNA, which encodes the GABA synthesizing enzyme glutamate decarboxylase. *GAD* expression was first detected at 24 hpf, in one to two cells located within the developing neural tube (Fig. A2a,a'). Three distinct *GAD*-expressing cell clusters became visible in the CNS of early larvae at 30 hpf (Fig. A2b,b'). By 36 hpf, *GAD* was further expressed in isolated ectodermal cells (Fig. A2c,c') and, at 60 hpf, many additional *GAD*-expressing cells appeared along the CNS, in a zone posterior to the third *GAD* cell cluster (Fig. A2d,d',e,e'), as well as around the mouth (Fig. A2d,d',e,e'). Changing RA signaling levels at 6 hpf affected *GAD*-expressing cells in amphioxus larvae at 36 and 60 hpf in the same way as GABA-ir neurons (compare Fig. A2 with Figs. 5 and 6). Of note, no effect of BMS493 or RA treatments could be discerned for *GAD*-expressing cells that appeared during later larval development (60 hpf) along the neural tube posterior to the initial three *GAD* cell clusters (Fig. A2 f-k,f'-k'). Also, *GAD* expression in the ectoderm and oral region of 60 hpf larvae was generally inconspicuous, precluding analysis of treatment phenotypes. Nonetheless, *B. lanceolatum GAD* expression corresponded well to that in *B. floridae* [27] as well as to GABA-ir in *B. lanceolatum* (Fig. 4). Yet, the latter revealed significantly more cellular details, which correspond well to the wide distribution of GABA-ir in *B. lanceolatum* adults [51].

In sum, our data show that RA signaling serves several context-dependent functions during early amphioxus development. It patterns the hindbrain-like portion of the neural tube by limiting the number of GABA cluster containing segments as well as the anterior ectoderm by regulating the formation of both visceral GABA neurons and DA-ir neurons. Furthermore, RA signaling promotes the GABAergic differentiation of ESNs in anterior ectoderm and influences neurite outgrowth.

Retinoic acid signaling-dependent patterning of neural cell populations corresponds to changes in *Hox* gene expression

In amphioxus, RA signaling mediates the regional patterning of the embryo by establishing collinear expression of *Hox* genes along the anterior-posterior body axis [36, 41]. We thus investigated whether RA-induced mispatterning of DA and GABA cell populations could be explained by concurrent changes in *Hox* gene expression. Noticeably, the anterior limit of ectodermal *Hox1* expression in control animals at 36 hpf coincided with the posterior limit of the DA-ir cell cluster (Fig. 7a,d,a'). Early treatments with BMS493, which caused a posterior expansion of the DA-ir cell cluster, induced a corresponding posterior shift of the anterior limit of *Hox1* expression (Fig. 7b,e,b'). Conversely, early RA treatments, which completely abolished DA-ir cells, simultaneously expanded the *Hox1* expression domain anteriorly (Fig. 7c,f,c'). These data suggest that RA signaling might define the posterior limit of the DA-ir cell cluster via modulation of *Hox1* expression in the ectoderm of amphioxus larvae. This hypothesis is supported by the facts that *Hox1* is a direct target of the RA signaling pathway of amphioxus [16] and that late BMS493 and RA treatments, at 24 hpf, when *Hox1* expression is already established [41], did not alter the number or position of DA-ir cells (Fig. 2).

Furthermore, we found a similar correlation between *Hox3* expression and GABA/*GAD* cell clusters in the anterior hindbrain of amphioxus larvae. At 30 and 36 hpf, GABA/*GAD* cell clusters were segmentally arranged at distances of 20-25 µm (Fig. 4b,c; Fig. A2b,c,b',c'). The same distance could further be observed between the posterior-most *GAD* cell cluster and the anterior expression limit of *Hox3*, which thus abutted the posterior limit of *GAD* cell-containing hindbrain segments (Fig. 7g,j,m,g',j'). Early BMS493 treatments, which led to the gain of additional GABA/*GAD* cell clusters at more posterior levels, concurrently shifted *Hox3* expression to a more posterior level (Fig. 7h,k,n,h',k'). Conversely, early RA treatments, which abolished posterior GABA/*GAD* cell clusters, resulted in a corresponding anterior shift of *Hox3* expression (Fig. 7i,l,o,i',l'). Importantly, however, both treatments did not affect the segmental spacing of 20-25 µm between the *Hox3* expression domain and the *GAD* cell clusters (Fig. 7m-o). Accordingly, RA signaling appears to set the posterior limit for GABA/*GAD* cell-containing segments in the developing amphioxus hindbrain by

controlling *Hox3* expression. This notion is also supported by the facts that *Hox3* is a direct target of the RA signaling pathway of amphioxus [16] and that late BMS493 and RA treatments, at 24 hpf, when *Hox3* expression is already established in the amphioxus CNS [41], did not affect the number of GABA/*GAD* cell clusters (Fig. 5; Fig. A2).

Based on these results, it seems likely that RA signaling establishes discrete limits for the specification of different neural cell populations by regulating the expression of individual *Hox* genes that serve distinct functions.

Retinoic acid signaling is required for acquisition of motor control in amphioxus larvae

Given that RA signaling influences the number and distribution of neurons in both the CNS and PNS during amphioxus development, we last tested whether it also affects larval locomotion. To assess how the animals flex their bodies during muscular swimming, we analyzed slow motion videos of amphioxus larvae at 60 hpf (Fig. 8; Online Resource 2). Controls bent their body sideways on average producing a maximum inner curvature (MIC) of 6.52 mm^{-1} (σ=0.54) (n=10) (Fig. 8; Online Resource 2). BMS493-treated larvae alternated left-right bends properly, but their movements appeared shallower. If exposed to BMS493 at 6 hpf, the animals bent with a significantly lower MIC of 4 mm^{-1} (σ=0.31) (n=10), while late BMS493 treatments at 24 hpf did not reduce larval bending motions significantly, with an average MIC of 6.37 mm^{-1} (σ=0.97) (n=10). In comparison, following early RA treatments at 6 hpf, amphioxus larvae were incapable of muscular swimming, but displayed disconnected twitches during which they bent their bodies much further than controls, reaching an average MIC of 18.39 mm^{-1} (σ=10.51) (n=10). As a result, their rostral and caudal ends often crossed each other. In response to later RA treatments at 24 hpf, amphioxus larvae were capable of muscular swimming, but still exhibited exaggerated bending motions, with an average MIC of 28.31 mm^{-1} (σ=21.8) (n=10). Instead of alternating left-right bends like control animals, RA-treated larvae further had a tendency to bend themselves several times towards the same side, especially for early treatments at 6 hpf. In sum, our results thus indicate that RA

signaling is required for establishing motor control in amphioxus larvae, including left-right coordination and intensity regulation of muscular contraction.

Discussion

Context-dependent retinoic acid signaling functions during establishment of neural cell populations in amphioxus

This study provides a detailed description of how RA signaling affects the development of 5-HT, DA, and GABA cell populations as well as motor control in amphioxus larvae (for an overview, see Table 1). 5-HT neurons can typically be observed within the apical ganglion of lophotrochozoan and non-vertebrate deuterostome larvae [59]. Consistently, a small cluster of 5-HT neurons has previously been detected in the frontal eye complex of the Florida amphioxus, *B. floridae* [27], and the Japanese amphioxus, *B. japonicum* [32]. Here we show that larvae of the European amphioxus, *B. lanceolatum*, possess a corresponding cluster of 5-HT-ir neurons. According to [59], 5-HT neurons found within the apical ganglion of non-vertebrate deuterostome larvae might be evolutionary related to hindbrain 5-HT neurons of the vertebrate raphe-system. Along the ventral hindbrain and spinal cord of vertebrates, low versus high RA signaling levels have been shown to respectively determine 5-HT versus glutamatergic neuronal fates [7, 8]. However, changing RA signaling levels did not affect 5-HT-ir neurons in the anterior CV of amphioxus larvae. This is probably due to presence of the RA-degrading enzyme CYP26 and the competitive RAR-inhibitor TR2/4 in the anterior-most portion of the amphioxus neural plate and neural tube [45, 47]. Nonetheless, early exposure to excess RA slightly disorganized TH-ir neurons and prevented neurite outgrowth from GABA-ir neurons at the posterior limit of the CV, suggesting that a sharp boundary for RA sensitivity exists in this area. Analyses of marker gene expression indicate that the posterior limit of the amphioxus CV represents, indeed, an important anterior-posterior landmark that might be equivalent to the vertebrate midbrain-hindbrain boundary [16, 25, 26, 60]. Since RA is also absent from forebrain and midbrain regions of early vertebrate embryos [61–64], our observations support homology of the 5-HT neurons found in the amphioxus frontal eye complex with

either vertebrate retinal ganglion cells or 5-HT cells of the pineal organ of lamprey embryos, rather than with 5-HT neurons of the vertebrate hindbrain [32, 49, 65].

Neural Cell Populations		**Pharmacological Treatment Effects**			
Neurochemistry	**Location**	**t:6 BMS493**	**t:24 BMS493**	**t:6 RA**	**t:24 RA**
5-HT	Anterior CV	0	0	0	0
TH	Posterior CV	0	0	d	0
DA + TH	Right Papilla	+	+/0	-	-/0
GABA	Hindbrain	+	0	-	-/0
GABA	Lateral Ectoderm	-	0	0	0
GABA	Oral Plexus	+/d	d/0	-/d	-/0
Bending Motions		reduced	normal	excessive	excessive

Table 1 Summary of the results obtained from immunohistochemical analyses following pharmacological treatments of developing amphioxus with the retinoic acid receptor (RAR) antagonist BMS493 or all-*trans* retinoic acid (RA). The effects on the formation of selected neural cell populations and on motor control are indicated. The developmental time point (t:) of the treatment, at either 6 or 24 hpf (hours post fertilization), is given together with the compound. Treatment outcomes for the different neural populations are depicted as follows: 0 = no effect, d = disruption of cell arrangement and/or morphology, + = gain of cells, - = loss of cells. Minor effects are indicated with a "/0". Abbreviations: 5-HT – serotonin, BMS493 – retinoic acid receptor antagonist, CV – cerebral vesicle, DA – dopamine, GABA – γ-aminobutyric acid, RA – retinoic acid, TH – tyrosine hydroxylase.

The neurotransmitter DA modulates behavior in all animal phyla studied so far, ranging from cnidarians to humans [54]. In vertebrates, DA is widely distributed throughout the entire CNS and can further be released by sympathetic nerves, chromaffin cells of the adrenal medulla, retinal cells, and neuroendocrine cells in the

kidney and pancreas [55, 66, 67]. Although presence of DA-ir neurons in the CNS of adult amphioxus has been demonstrated [50], we could detect DA-ir only in a single ectodermal cell cluster of the amphioxus larva. This could be due to technical issues like photo-oxidation [50], but rearing, fixing, and staining animals in the dark did not yield additional signal (data not shown). Notably, we could detect the DA synthesis enzyme TH not only in cells of the DA-ir cell cluster but also in other tissues, including neurons of the posterior CV. These neurons might adopt their full DA-ir phenotype at later developmental stages or might use the DA precursor L-DOPA rather than actual DA as a neurotransmitter [68–70]. In addition, most of the peripheral TH-ir cells we observed probably produce pigment rather than DA [71–73]. Since TH/DA-ir cells of the right papilla are large and lack neurites, they are probably neurosecretory. Their position near the endostyle and a mucus gland as well as the timing of their appearance, shortly before the larval mouth opens, indicate a role in regulating feeding behavior, which is a well-conserved function of DA signaling [54]. This notion is supported by strong expression of an amphioxus DA receptor throughout the endostyle of *B. floridae* larvae [56]. Interestingly, DA-ir can also be observed in cutaneous adhesive papillae of young tunicate larvae as well as in the endostyle and near the newly formed pharynx of metamorphosing tunicate juveniles [74, 75]. Hence, DA signaling in the oral region and specialized structures of the head ectoderm seems to be a shared feature of the larvae of non-vertebrate chordates.

It has been suggested that TH might be a direct target of the vertebrate RA signaling pathway, since RAR can robustly trans-activate TH promoter function in a ligand-dependent manner [76]. However, RA signaling appears to exert opposite effects on TH gene expression, depending on the cell type [9, 10, 76]. During early amphioxus development, increasing or inhibiting RA signaling respectively caused the loss or the posterior expansion of an ectodermal DA-ir cell cluster. Yet, altering RA signaling levels at later developmental stages produced weaker or no apparent phenotypes and the formation of TH-ir neurons in the amphioxus CV was largely independent of RA signaling levels. Given these findings, we conclude that the amphioxus RA signaling pathway does not affect DA synthesis directly, but instead plays an early developmental role in patterning the anterior ectoderm by restricting the specification of DA-ir cells.

Importantly, we observed a similar mode of RA signaling action during the establishment of GABA-ir cell clusters in the hindbrain homolog of amphioxus larvae. Exposure to excess RA eliminated posterior GABA-ir cell clusters, while inhibition of RA signaling resulted in the formation of additional GABA-ir cell clusters at more posterior levels. Again, this effect was only observable, if RA signaling levels were manipulated at early developmental stages. Moreover, RA signaling had no apparent influence on late developing GABA-ir neurons in more posterior portions of the larval neural tube. Therefore, we propose that RA signaling does not affect GABA synthesis directly in amphioxus, but rather patterns the hindbrain territory by limiting the number of GABA cluster-containing segments that can become specified during early embryogenesis. Notably, this function is exerted in parallel to the observed RA signaling-dependent patterning of anterior ectoderm, which ensures proper formation of both the DA-ir cell cluster and visceral GABA-ir neurons of the oral plexus. These data are in agreement with the broad involvement of RA signaling in patterning the hindbrain, the spinal cord, and various neural crest as well as cranial placode derivatives in vertebrates [77].

Antagonizing RA signaling at early developmental stages also significantly reduced the number of GABA-ir ESNs in the anterior ectoderm. This was likely due to a change of neurotransmitter identity, since counterstaining with an antibody against the neuronal marker acetylated tubulin revealed no concomitant decrease in the overall number of ESNs (data not shown). During early amphioxus development, low levels of RA signaling might thus be required in the anterior PNS to promote GABAergic fates. This is in agreement with studies reporting that RA treatments can be used for the efficient and scalable generation of functional GABAergic interneurons from embryonic stem cells [78–80]. In vertebrates, RA was further shown to contribute to the specification and differentiation of both GABA neurons in the basal ganglia [11] and a neuronal cell population that co-releases DA and GABA in the substantia nigra [10, 81]. These results indicate that RA signaling plays a well-conserved role in promoting GABAergic differentiation in chordates, albeit in a strictly context-dependent manner.

Finally, we found that altering RA signaling levels specifically perturbs the formation of caudal projections, for instance from GABA-ir cell clusters in the

hindbrain and from GABA-ir neurons in the oral plexus. Since both exposure to excess RA and blocking of RA signaling would mask a posterior-high RA signaling gradient, it can be assumed that RA provides graded cues to regulate the outgrowth of caudal projections in amphioxus larvae. This hypothesis is consistent with the central role RA plays during neurite outgrowth and axonal elongation in vertebrates [82]. Taken together, our results illustrate how RA signaling acts in a stage- and tissue-specific manner to control the formation of distinct neural cell populations in amphioxus larvae and highlight that these functions are largely conserved in chordates.

Evolution of retinoic acid signaling and *Hox* gene interactions during nervous systems development: insights from amphioxus

It is known that RA signaling patterns the CNS of both vertebrates [3, 63] and amphioxus [41, 47, 63] by modulating the collinear expression of *Hox* genes. RA signaling and *Hox* gene interactions might further be required for establishing the PNS of chordates. For instance, RA signaling has been implicated in the development of vertebrate neural crest and neurogenic placodes, including the olfactory placode, the adenohypophyseal placode, and the otic placode [77]. Interestingly, the latter is considered homologous to the atrial siphon placode of the tunicate *C. intestinalis*, which requires RA-induced *Hox1* expression for its proper formation [19]. Furthermore, it has been shown that RA signaling influences the distribution of amphioxus ESN progenitors as well as their expression of *Hox* and pro-neural genes [36]. *Hox* genes hence appear to be important mediators of RA signaling functions in patterning both CNS and PNS structures of chordates.

In most vertebrate genomes, *Hox* genes are organized in linked clusters of up to 11 genes on four chromosomes [83]. In contrast, amphioxus possesses only a single *Hox* cluster comprising a full complement of 15 *Hox* genes [42, 84]. So far, only *Hox1* and *Hox3* are confirmed direct target genes of the amphioxus RA signaling pathway [16]. Consistently, our findings suggest that RA signaling restricts the formation of DA-ir cells in the ectoderm and GABA-ir cell clusters in the CNS of amphioxus larvae, through respective regulation of *Hox1* and *Hox3* expression (Fig.

9). This hypothesis is in agreement with previous research showing that the RA signaling-dependent expression of *Hox1* is also responsible, during amphioxus development, for determining the posterior limit of the pharynx and for controlling its segmentation [47, 85, 86]. Concomitantly, we found that RA treatments abolish the independent network of ectodermal GABA-ir neurons, which normally innervates the mouth and gill slits. Thus, the amphioxus RA signaling pathway seems to contribute simultaneously to the patterning of the endodermal pharynx, the ectodermal GABA-ir oral plexus, and the ectodermal DA-ir cell cluster, via regulation of *Hox1* gene function, as well as to the patterning of GABA-ir cell clusters in the CNS, via regulation of *Hox3* gene function. This is comparable to the situation in vertebrates, where RA is used as a major trunk organizing signal across all tissue layers [87, 88].

However, our observations indicate that, contrary to the combinatorial mode of *Hox* gene function in vertebrates [89–93], amphioxus *Hox* genes probably act independently to serve distinct roles. A potential explanation for this difference lies in the structural organization of cephalochordate versus vertebrate *Hox* gene clusters. The genomic regions of vertebrate *HoxA* and *HoxD* clusters, for instance, are each divided into two adjacent three-dimensional chromatin structures that separate long-range regulatory inputs coming from regions neighboring the anterior 3' *Hox* genes and the posterior 5' *Hox* genes [94]. In vertebrates, *Hox* gene expression is thus regulated by both RA signaling, which modifies the chromatin domains of anterior 3' *Hox* genes to induce their expression [3, 92], and CDX transcription factors, which remove repressive chromatin modifications from posterior 5' *Hox* genes to enable their transcriptional activation via FGF and WNT signaling [3, 92, 95].

The amphioxus *Hox* cluster, on the other hand, is organized into only a single chromatin interaction domain that mostly includes long-range contacts from the anterior 3' side [96]. Accordingly, transcription of several amphioxus *Hox* genes is also directly controlled by RA signaling [16, 97], but FGF signaling appears to be much less important for posterior development in amphioxus than in vertebrates [98, 99]. A bipartite regulatory network of *Hox* clusters, which allows switching between two sets of long-range regulatory inputs to increase the plasticity of *Hox* gene action during development, hence seems to be an evolutionary novelty of vertebrates [96]. Furthermore, amphioxus *Hox* gene promoters lack *Krox20* and *Kreisler*/*Mafb*

response elements as well as several binding sites mediating *Hox* auto- and cross-regulatory inputs [100]. Together, these findings suggest that, compared to vertebrates, the *Hox* genes of ancestral chordates were regulated in a more straightforward and individual manner, thus serving mostly independent roles instead of participating in a holistic combinatorial *Hox* code. The latter might have evolved as a consequence of whole genome duplications in the vertebrate lineage, which were associated with a considerable elaboration of the *Hox* regulatory landscape controlling both cluster-wide and gene-specific transcriptional activity [43, 90, 91].

Retinoic acid signaling is required for the acquisition of motor control

Misregulation of RA signaling levels during vertebrate development can be linked to various neurobehavioral effects, such as hyperactivity and motor impairments [101–104]. By capturing slow motion movies of swimming larvae, we were able to show that RA signaling is also crucial for the acquisition of motor control in *B. lanceolatum*. RA signaling-induced motor impairments have so far mainly been attributed to disruptions of vertebrate DA and cholinergic systems [101, 105, 106]. In contrast, our results in amphioxus strongly suggest that RA signaling-dependent motor defects are, at least in part, caused by disruptions of the hindbrain GABAergic system. Widely distributed throughout both vertebrate and non-vertebrate nervous systems, the inhibitory neurotransmitter GABA is known to reduce neuronal excitability, which is particularly important for the control of motor functions [107–109]. For instance, GABA neurotransmission ensures the precision and smoothness of vertebrate locomotion by shaping the response of motor neurons to excitatory inputs [110, 111] and is crucial for the coordination of larval swimming in tunicates [112, 113]. In amphioxus, GABA-ir neurons are initially restricted to three cell clusters in the anterior neural tube that differentiate already at early larval stages, when the animals start to exhibit their first muscular contractions. The anterior-most of these GABA-ir cell clusters is located at the posterior limit of the CV, in close proximity to the primary motor center [28]. Accordingly, GABAergic inhibition might also conduce the undulatory swimming motion of amphioxus larvae. Notably, we observed GABA-ir neurites crossing to the contra-lateral side of the neural tube just posterior to each of the initial three GABA-ir cell clusters. These neurites likely inhibit the contraction of

opposite somites along the larval body to coordinate sequences of bends and counter-bends. This hypothesis is in agreement with studies reporting that GABA-mediated reciprocal inhibition is required for alternated left-right limb movement in vertebrates [114] and that reducing GABA neurotransmission in tunicates perturbs left-right alternation during larval swimming [113]. Accordingly, the GABAergic systems of amphioxus and tunicate larvae, despite being composed of only a few neurons, appear to serve similar functions as the much more complex GABAergic circuitry of vertebrates.

When amphioxus embryos were exposed to excess RA during early development, their larval muscular contractions were significantly more intense than in control animals. This phenotype was associated with a loss of posterior GABA-ir cell clusters and projections within the hindbrain. In contrast, early inhibition of RA signaling reduced larval muscular contractions and simultaneously increased the number of hindbrain GABA cell clusters. Accordingly, a lack of GABA-mediated inhibition versus excessive GABAergic inhibition of amphioxus motor circuits might be responsible, respectively, for the observed exaggeration and suppression of larval bending motions in amphioxus. Correspondingly, GABA antagonists generally act as convulsants [115], whereas agonists of GABA receptors typically induce muscle relaxation and sedation in vertebrates [116, 117]. GABA exposure has further been shown to completely immobilize tunicate larvae [112] and, in humans, elevating GABA neurotransmission through alcohol consume is known to trigger a general decrease of neuronal excitability that impairs both sensory and motor functions [118]. Therefore, RA signaling-dependent formation of GABAergic neurons might be important for establishing motor control in all three chordate subphyla. Surprisingly, however, late RA treatments, at 24 hpf, also led to more intense muscular contractions in amphioxus larvae, even though they only reduced GABA-ir neurite outgrowth along the CNS, without altering the overall number of GABA-ir cell clusters. This indicates that the efficient attenuation of larval bending movements relies on the far-reaching caudal projections of the GABA-ir cell clusters, which likely prevent excessive contraction of posterior somites.

Following RA-treatments, the swimming motion of amphioxus larvae was also poorly coordinated. Rather than alternating left-right bends properly, the animals

often bent several times towards the same side. This finding is in line with studies reporting a requirement of reciprocal GABA inhibition for left-right alternate movements in vertebrates as well as in tunicate larvae [113, 114]. Furthermore, early RA treatments affected the coordination of left-right bends in amphioxus larvae more strongly than late RA treatments, supporting the notion that this process involves the crossing neurites just posterior to each of the three GABA-ir cell clusters, since two of them are lost in response to early but not late RA treatments. In sum, these data highlight the importance of RA signaling for establishing motor control systems by patterning GABA cell clusters in the hindbrain of amphioxus larvae. Comparisons with tunicates and vertebrates support an evolutionary conservation of these functions among chordates, which highlights the usefulness of comparative approaches for studying RA and GABA signaling-related neurological processes.

Materials and Methods

Animals

Adult specimens of the European amphioxus, *B. lanceolatum*, were collected from sand samples retrieved in Argelès-sur-Mer, France. About ten animals were kept in 5 l aquaria with a seawater temperature of 16 to 17ºC and a periodical light cycle of 14 h light and 10 h darkness. To induce spawning, males and females with mature gonads were selected and exposed to a 36 h thermal shock at 23ºC, as previously described [119–121]. From each female, several hundred oocytes were collected in a petri dish. After successful *in vitro* fertilization, as indicated by the expansion of a fertilization envelope, the developing zygotes were incubated in artificial seawater at 19°C in the dark [122].

Pharmacology

Embryos of *B. lanceolatum* were treated with all-*trans* RA at a final concentration of 0.1 µM or with the RAR antagonist BMS493 at a final concentration of 1 µM. Both compounds were purchased from Sigma-Aldrich (Saint-Quentin Fallavier, France) and were dissolved in dimethyl sulfoxide (DMSO) to create 1000X stock solutions, which were added to *B. lanceolatum* embryo cultures to yield the respective final concentrations. In addition, control cultures were treated with DMSO at a final concentration of 1:1000 [47]. Pharmacological treatments were initiated either at late blastula (6 hpf), mid-gastrula (12 hpf), mid-neurula (24 hpf), feeding larva (36 hpf) or late feeding larva (48 hpf) stages.

Behavioral analyses

B. lanceolatum larvae at 60 hpf were transferred into a Petri dish containing 10 ml of artificial seawater and placed under a stereomicroscope. Their swimming movements were filmed at a speed of 200 frames/sec using a Hamamatsu Flash4 camera. In order to induce muscular swimming, the Petri dish containing the *B. lanceolatum* larvae was agitated occasionally. Videos were analyzed with the ImageJ software [123] and exported at a speed of 5 frames/sec. The maximum inner curvature (MIC) was determined with the ImageJ software [123]: a circle was fitted into the most curved part of a larva in the maximum bending position and the radius

(r) of this circle was subsequently measured. The MIC was then calculated as $\kappa=1/r$. Ten amphioxus larvae were measured per treatment condition and statistical significance was tested using a two-tailed student's t-test assuming unequal variances.

Gene cloning

The sequence for glutamate decarboxylase (*GAD*) was identified in the *B. lanceolatum* transcriptome through BLAST searches using the human *GAD1* (NP_000808.2) and *GAD2* (NP_001127838.1) sequences as queries [124]. The obtained *B. lanceolatum GAD* sequence was next translated into an amino acid sequence and aligned with its orthologs from human (*Homo sapiens*) (*GAD1*: NP_000808.2; *GAD2*: NP_001127838.1), chicken (*Gallus gallus*) (*GAD1*: NP_990244.1; *GAD2*: XP_015137540.1), sea urchin (*Strongylocentrotus purpuratus*) (*GAD*: XP_011664015.1), fruit fly (*Drosophila melanogaster*) (*GAD*: NP_523914.2), red flour beetle (*Tribolium castaneum*) (*GAD*: XP_974463.1), and Florida amphioxus (*B. floridae*) (*GAD*: XP_002592141.1), using the MUSCLE program [125] with default parameters. Residues in the alignment with more than 75% gaps were removed using the –gt=0.25 parameter from TrimAl v1.2 [126]. The *GAD* alignment comprising 593 positions was used to infer a maximum likelihood (ML) phylogeny using RAxML with 1000 rapid bootstraps [127]. The best-suited model for this alignment (LG+Γ+I) was determined using Protest v3.4 [128]. The resulting tree validated the *B. lanceolatum* sequence as a true *GAD* homolog (data not shown).

Subsequently, RNA was extracted from embryos at different developmental stages (18 hpf, 24 hpf, 36 hpf, and 48 hpf) and cDNA was synthesized using the SuperScriptIII reverse transcription kit from Invitrogen (Cergy Pontoise, France) according to established protocols [129]. The open reading frame of the *B. lanceolatum GAD* (KY242584) was amplified by polymerase chain reaction (PCR), using the gene-specific primers 5'-CAGTCACCCGGCTCCTATAAACAACACTAG-3' and 5'-CAAGTCTTCTCCTAGCCGTTCTATCTCCTC-3'. In addition to the *B. lanceolatum GAD* gene, the *B. lanceolatum Hox1* (EU921831) [130] and *Hox3* (EU921831) [130] clones used in this study were amplified by PCR using the following gene-specific primers: 5'-AATGAACTCGTACGTGGACT-3' and 5'-TGTTTCATCCTACGGTTCTG-3' for *Hox1*, 5'-ATGCAAAAATCACCTTACTACGA-3'

and 5'-TTCTGTTCTTTCTTATACTTCAT-3' for *Hox3*. All PCR products were cloned into the pGEM®T Easy Vector System from Promega and validated by sequencing on both DNA strands.

In situ hybridization and immunohistochemistry

For whole mount *in situ* hybridization and immunohistochemistry, *B. lanceolatum* embryos and larvae at different developmental stages were fixed in freshly prepared, ice cold 4% paraformaldehyde diluted in MOPS buffer [131]. For GABA immunohistochemistry, 0.3% glutaraldehyde was added to the fixative. For *in situ* hybridization, antisense riboprobes were synthesized and *in situ* hybridization experiments were carried out as previously described [131]. Double *in situ* hybridization was performed according to published protocols [132], using a *Hox3* riboprobe labeled with fluorescein (Roche) and a *GAD* riboprobe labeled with digoxigenin (Roche), which were detected, respectively, with an anti-fluorescein antibody conjugated with alkaline phosphatase and an anti-digoxigenin antibody conjugated with alkaline phosphatase from Roche. For the first color reaction (*Hox3*), nitroblue tetrazolium/5-bromo-4-chloro-3-indolyl phosphate (NBT/BCIP) from Roche was used and for the second color reaction (*GAD*) a Fast Red RC tablet from Sigma-Aldrich was used.

For immunohistochemistry, fixed embryos were transferred into the wells of a 96-well plate and washed in several changes of PBS (phosphate buffered saline, 0.1 M, pH 7) for 1 h, followed by a pre-incubation in PBS-TX (PBS plus 0.3% Triton X-100) for 1 h. Next, the embryos were incubated in primary antibodies diluted in PBS-TX. All embryos were stained for acetylated tubulin (Sigma-Aldrich T6793, concentration 2:1000) and either DA (Abcam ab8888, concentration 2:1000, for 72 h at 4°C), TH (Millipore AB152, concentration 4:1000, for 72 h at 4°C), 5-HT (ImmunoStar 20080, concentration 3:1000, for 12 h at 22°C) or GABA (Abcam ab8891 concentration 3:1000, for 12 h at 22°C). The primary antisera were washed off with several changes of PBS for 2 h and the embryos were then incubated in the secondary antibodies anti-rabbit IgG Alexa Fluor®488 (Thermo Fisher Scientific A-11008, concentration 3:1000) and anti-mouse Cy3™ (Bethyl Laboratories Inc. A90-516C3, concentration 3:1000) as well as in the nucleic acid dye Hoechst (bisBenzimide, Invitrogen, concentration 1:5000) diluted in PBS for 12 h at 4°C.

Subsequently, the embryos were washed once more for 2 h in several changes of PBS and mounted in Mowiol (Sigma-Aldrich).

Imaging and image analyses

Images of *B. lanceolatum* embryos after *Hox1*, *Hox3*, and *GAD* single *in situ* hybridization were taken as whole mounts using Zeiss differential interference contrast optics (Carl Zeiss SAS, Marly le Roi, France). After double *in situ* staining for *Hox3* and *GAD*, the embryos were imaged with a Leica TCS SP5 confocal microscope (Leica Microsystems SAS, Nanterre, France). The NBT/BCIP signal was excited at 633 nm (HeNe laser) and detected at 660-680 nm, while the Fast Red signal was excited at 514 nm (Argon laser) and detected at 560-600 nm. For immunostained embryos, the Cy3™ signal was excited at 543 nm (HeNe laser) and detected at 560-580 nm, the Alexa Fluor®488 signal was excited at 488 nm (Argon laser) and detected at 515-540 nm and the Hoechst signal was excited at 405 nm (UV laser diode) and detected at 430-460 nm. Series of optical sections were taken at a z-step interval of 0.8 µm. The ImageJ software [123] was subsequently used for image processing and to generate maximum as well as 3D projections. Cell numbers were counted manually and statistical significance ($p<0.05$) was assessed using Welch's t-test (two-tailed student's t-tests assuming unequal variances).

Acknowledgments

The Observatoire Océanologique de Banyuls-sur-Mer in Banyuls-sur-Mer, France, kindly provided *Branchiostoma lanceolatum* adults, and Hector Escriva graciously coordinated and supported the animal collections. The authors are grateful to Thurston C. Lacalli, Jr-Kai Yu, Nicholas D. Holland, Linda Z. Holland, and Ievgeniia Gazo for fruitful discussions. We would also like to thank Ram Reshef for his vital support in administrative issues.

Funding

This work was supported by a grant from the Agence Nationale de la Recherche (ANR-11-JSV2-002-01) and by funds from the Réseau André Picard (ANR-11-IDEX-0004-02, Sorbonne Universities) to MS and by a National Grant of the University of Genoa, Italy (2015) to SC. EZ was a doctoral fellow of the Studienstiftung der Deutschen Wirtschaft (SDW).

Competing interests

The authors declare that they have no competing interests.

References

1. Chambon P (1996) A decade of molecular biology of retinoic acid receptors. FASEB J 10:940–954.
2. Moutier E, Ye T, Choukrallah M-A, et al (2012) Retinoic acid receptors recognize the mouse genome through binding elements with diverse spacing and topology. J Biol Chem 287:26328–26341. doi: 10.1074/jbc.M112.361790
3. Mazzoni EO, Mahony S, Peljto M, et al (2013) Saltatory remodeling of *Hox* chromatin in response to rostrocaudal patterning signals. Nat Neurosci 16:1191–1198. doi: 10.1038/nn.3490
4. Duester G (2013) Retinoid signaling in control of progenitor cell differentiation during mouse development. Semin Cell Dev Biol 24:694–700. doi: 10.1016/j.semcdb.2013.08.001
5. Gudas LJ (2013) Retinoids induce stem cell differentiation via epigenetic changes. Semin Cell Dev Biol 24:701–705. doi: 10.1016/j.semcdb.2013.08.002
6. Janesick A, Wu SC, Blumberg B (2015) Retinoic acid signaling and neuronal differentiation. Cell Mol Life Sci. doi: 10.1007/s00018-014-1815-9
7. Jacob J, Kong J, Moore S, et al (2013) Retinoid acid specifies neuronal identity through graded expression of *Ascl1*. Curr Biol 23:412–418. doi: 10.1016/j.cub.2013.01.046
8. Carcagno AL, Di Bella DJ, Goulding M, et al (2014) *Neurogenin3* restricts serotonergic neuron differentiation to the hindbrain. J Neurosci 34:15223–15233. doi: 10.1523/JNEUROSCI.3403-14.2014
9. Jacobs FMJ, Smits SM, Noorlander CW, et al (2007) Retinoic acid counteracts developmental defects in the substantia nigra caused by *Pitx3* deficiency. Dev Camb Engl 134:2673–2684. doi: 10.1242/dev.02865
10. Jacobs FMJ, Veenvliet JV, Almirza WH, et al (2011) Retinoic acid-dependent and -independent gene-regulatory pathways of *Pitx3* in meso-diencephalic dopaminergic neurons. Development 138:5213–5222. doi: 10.1242/dev.071704
11. Chatzi C, Brade T, Duester G (2011) Retinoic acid functions as a key GABAergic differentiation signal in the basal ganglia. PLoS Biol 9:e1000609. doi: 10.1371/journal.pbio.1000609
12. Carter CJ, Rand C, Mohammad I, et al (2015) Expression of a retinoic acid receptor (RAR)-like protein in the embryonic and adult nervous system of a protostome species. J Exp Zoolog B Mol Dev Evol 324:51–67. doi: 10.1002/jez.b.22604
13. Carter CJ, Farrar N, Carlone RL, Spencer GE (2010) Developmental expression of a molluscan RXR and evidence for its novel, nongenomic role in growth cone guidance. Dev Biol 343:124–137. doi: 10.1016/j.ydbio.2010.03.023
14. Farrar NR, Dmetrichuk JM, Carlone RL, Spencer GE (2009) A novel, nongenomic mechanism underlies retinoic acid-induced growth cone turning. J Neurosci 29:14136–14142. doi: 10.1523/JNEUROSCI.2921-09.2009
15. Fuchs B, Wang W, Graspeuntner S, et al (2014) Regulation of polyp-to-jellyfish transition in *Aurelia aurita*. Curr Biol 24:263–273. doi: 10.1016/j.cub.2013.12.003
16. Koop D, Holland ND, Sémon M, et al (2010) Retinoic acid signaling targets *Hox* genes during the amphioxus gastrula stage: insights into early anterior–posterior patterning of the chordate body plan. Dev Biol 338:98–106. doi: 10.1016/j.ydbio.2009.11.016
17. Pasini A, Manenti R, Rothbächer U, Lemaire P (2012) Antagonizing retinoic acid and FGF/MAPK pathways control posterior body patterning in the invertebrate chordate *Ciona intestinalis*. PLoS ONE 7:e46193. doi: 10.1371/journal.pone.0046193
18. Pennati R, Dell'Anna A, Zega G, et al (2013) Retinoic acid influences antero-posterior positioning of peptidergic neurons in the planula larva of the hydrozoan *Clava multicornis*. Mar Ecol 34:143–152. doi: 10.1111/maec.12032

19. Sasakura Y, Kanda M, Ikeda T, et al (2012) Retinoic acid-driven *Hox1* is required in the epidermis for forming the otic/atrial placodes during ascidian metamorphosis. Development 139:2156–2160. doi: 10.1242/dev.080234
20. Laudet V, Zieger E, Schubert M (2015) Evolution of the retinoic acid signaling pathway. In: Dollé P, Neiderreither K (eds) The retinoids. John Wiley & Sons, Inc, Hoboken, NJ, pp 75–90
21. Delsuc F, Tsagkogeorga G, Lartillot N, Philippe H (2008) Additional molecular support for the new chordate phylogeny. genesis 46:592–604. doi: 10.1002/dvg.20450
22. Yue J-X, Yu J-K, Putnam NH, Holland LZ (2014) The transcriptome of an amphioxus, *Asymmetron lucayanum*, from the Bahamas: a window into chordate evolution. Genome Biol Evol 6:2681–2696. doi: 10.1093/gbe/evu212
23. Bourlat SJ, Juliusdottir T, Lowe CJ, et al (2006) Deuterostome phylogeny reveals monophyletic chordates and the new phylum Xenoturbellida. Nature 444:85–88. doi: 10.1038/nature05241
24. Carvalho JE, Schubert M (2013) Retinoic acid: metabolism, developmental functions and evolution. Vitam.-Bind. Proteins Funct. Consequences
25. Holland LZ (2015) The origin and evolution of chordate nervous systems. Philos Trans R Soc B Biol Sci 370:20150048–20150048. doi: 10.1098/rstb.2015.0048
26. Holland LZ, Carvalho JE, Escriva H, et al (2013) Evolution of bilaterian central nervous systems: a single origin? EvoDevo 4:27. doi: 10.1186/2041-9139-4-27
27. Candiani S, Moronti L, Ramoino P, et al (2012) A neurochemical map of the developing amphioxus nervous system. BMC Neurosci 13:59.
28. Wicht H, Lacalli TC (2005) The nervous system of amphioxus: structure, development, and evolutionary significance. Can J Zool 83:122–150. doi: 10.1139/z04-163
29. Castro A, Becerra M, Manso MJ, Anadón R (2015) Neuronal organization of the brain in the adult amphioxus *Branchiostoma lanceolatum*: a study with acetylated tubulin immunohistochemistry. J Comp Neurol 523:2211–2232. doi: 10.1002/cne.23785
30. Lacalli TC (2013) Looking into eye evolution: amphioxus points the way. Pigment Cell Melanoma Res 26:162–164. doi: 10.1111/pcmr.12057
31. Lacalli TC (1996) Frontal eye circuitry, rostral sensory pathways and brain organization in amphioxus larvae: evidence from 3D reconstructions. Philos Trans R Soc B Biol Sci 351:243–263. doi: 10.1098/rstb.1996.0022
32. Suzuki DG, Murakami Y, Escriva H, Wada H (2015) A comparative examination of neural circuit and brain patterning between the lamprey and amphioxus reveals the evolutionary origin of the vertebrate visual center: visual system in lampreys and amphioxus. J Comp Neurol 523:251–261. doi: 10.1002/cne.23679
33. Albuixech-Crespo B, López-Blanch L, Burguera D, et al (2017) Molecular regionalization of the developing amphioxus neural tube challenges major partitions of the vertebrate brain. PLOS Biol 15:e2001573. doi: 10.1371/journal.pbio.2001573
34. Zieger E, Lacalli TC, Pestarino M, et al (in press) The origin of dopaminergic systems in chordate brains: insights from amphioxus. Int. J. Dev. Biol.
35. Lu T-M, Luo Y-J, Yu J-K (2012) BMP and Delta/Notch signaling control the development of amphioxus epidermal sensory neurons: insights into the evolution of the peripheral sensory system. Development 139:2020–2030. doi: 10.1242/dev.073833
36. Schubert M, Holland ND, Escriva H, et al (2004) Retinoic acid influences anteroposterior positioning of epidermal sensory neurons and their gene expression in a developing chordate (amphioxus). Proc Natl Acad Sci 101:10320–10325. doi: 10.1073/pnas.0403216101
37. Meulemans D, Bronner-Fraser M (2007) The amphioxus *SoxB* family: implications for the evolution of vertebrate placodes. Int J Biol Sci 3:356–364.

38. Kaltenbach SL, Yu J-K, Holland ND (2009) The origin and migration of the earliest-developing sensory neurons in the peripheral nervous system of amphioxus. Evol Dev 11:142–151. doi: 10.1111/j.1525-142X.2009.00315.x
39. Lacalli TC (2004) Sensory systems in amphioxus: a window on the ancestral chordate condition. Brain Behav Evol 64:148–162. doi: 10.1159/000079744
40. Lacalli TC, Gilmour THJ, Kelly SJ (1999) The oral nerve plexus in amphioxus larvae: function, cell types and phylogenetic significance. Proc R Soc B Biol Sci 266:1461–1470. doi: 10.1098/rspb.1999.0801
41. Schubert M, Holland ND, Laudet V, Holland LZ (2006) A retinoic acid-*Hox* hierarchy controls both anterior/posterior patterning and neuronal specification in the developing central nervous system of the cephalochordate amphioxus. Dev Biol 296:190–202. doi: 10.1016/j.ydbio.2006.04.457
42. Putnam NH, Butts T, Ferrier DEK, et al (2008) The amphioxus genome and the evolution of the chordate karyotype. Nature 453:1064–1071. doi: 10.1038/nature06967
43. Holland LZ (2013) Evolution of new characters after whole genome duplications: insights from amphioxus. Semin Cell Dev Biol 24:101–109. doi: 10.1016/j.semcdb.2012.12.007
44. Holland LZ (2015) Genomics, evolution and development of amphioxus and tunicates: the Goldilocks principle. J Exp Zoolog B Mol Dev Evol 324:342–352. doi: 10.1002/jez.b.22569
45. Carvalho JE, Theodosiou M, Chen J, et al (2017) Lineage-specific duplication of amphioxus retinoic acid degrading enzymes (CYP26) resulted in sub-functionalization of patterning and homeostatic roles. BMC Evol Biol. doi: 10.1186/s12862-016-0863-1
46. Shimozono S, Iimura T, Kitaguchi T, et al (2013) Visualization of an endogenous retinoic acid gradient across embryonic development. Nature 496:363–366. doi: 10.1038/nature12037
47. Escriva H, Holland ND, Gronemeyer H, et al (2002) The retinoic acid signaling pathway regulates anterior/posterior patterning in the nerve cord and pharynx of amphioxus, a chordate lacking neural crest. Dev Camb Engl 129:2905–2916.
48. Candiani S, Augello A, Oliveri D, et al (2001) Immunocytochemical localization of serotonin in embryos, larvae and adults of the lancelet, *Branchiostoma floridae*. Histochem J 33:413–420.
49. Vopalensky P, Pergner J, Liegertova M, et al (2012) Molecular analysis of the amphioxus frontal eye unravels the evolutionary origin of the retina and pigment cells of the vertebrate eye. Proc Natl Acad Sci U S A 109:15383–15388. doi: 10.1073/pnas.1207580109
50. Moret F, Guilland J-C, Coudouel S, et al (2004) Distribution of tyrosine hydroxylase, dopamine, and serotonin in the central nervous system of amphioxus (*Branchiostoma lanceolatum*): implications for the evolution of catecholamine systems in vertebrates. J Comp Neurol 468:135–150. doi: 10.1002/cne.10965
51. Anadón R, Adrio F, Rodríguez-moldes I (1998) Distribution of GABA immunoreactivity in the central and peripheral nervous system of amphioxus (*Branchiostoma lanceolatum* Pallas). J Comp Neurol 401:293–307.
52. Van Wijhe JW (1925) On the temporary presence of the primary mouth-opening in the larva of amphioxus, and the occurrence of three postoral papillae, which are probably homologous with those of the larva of Ascidians. Proc K Ned Acad Van Wet 29:286–295.
53. Abalo XM, Villar-Cheda B, Anadón R, Rodicio MC (2005) Development of the dopamine-immunoreactive system in the central nervous system of the sea lamprey. Brain Res Bull 66:560–564. doi: 10.1016/j.brainresbull.2005.05.004
54. Barron AB, Søvik E, Cornish JL (2010) The roles of dopamine and related compounds in reward-seeking behavior across animal phyla. Front Behav Neurosci. doi:

10.3389/fnbeh.2010.00163
55. Smeets WJ, González A (2000) Catecholamine systems in the brain of vertebrates: new perspectives through a comparative approach. Brain Res Rev 33:308–379.
56. Candiani S, Oliveri D, Parodi M, et al (2005) *AmphiD1/beta*, a dopamine D1/beta-adrenergic receptor from the amphioxus *Branchiostoma floridae*: evolutionary aspects of the catecholaminergic system during development. Dev Genes Evol 215:631–638. doi: 10.1007/s00427-005-0019-6
57. Holland LZ, Holland ND (1996) Expression of *AmphiHox-1* and *AmphiPax-1* in amphioxus embryos treated with retinoic acid: insights into evolution and patterning of the chordate nerve cord and pharynx. Dev Camb Engl 122:1829–1838.
58. Lacalli TC, Hou S (1999) A reexamination of the epithelial sensory cells of amphioxus (*Branchiostoma*). Acta Zool 80:125–134. doi: 10.1046/j.1463-6395.1999.80220005.x
59. Hay-Schmidt A (2000) The evolution of the serotonergic nervous system. Proc R Soc B Biol Sci 267:1071–1079. doi: 10.1098/rspb.2000.1111
60. Castro LFC, Rasmussen SLK, Holland PWH, et al (2006) A *Gbx* homeobox gene in amphioxus: insights into ancestry of the ANTP class and evolution of the midbrain/hindbrain boundary. Dev Biol 295:40–51. doi: 10.1016/j.ydbio.2006.03.003
61. Cai AQ, Radtke K, Linville A, et al (2012) Cellular retinoic acid-binding proteins are essential for hindbrain patterning and signal robustness in zebrafish. Development 139:2150–2155. doi: 10.1242/dev.077065
62. del Corral R, Morales A (2014) Retinoic acid signaling during early spinal cord development. J Dev Biol 2:174–197. doi: 10.3390/jdb2030174
63. Glover JC, Renaud J-S, Rijli FM (2006) Retinoic acid and hindbrain patterning. J Neurobiol 66:705–725. doi: 10.1002/neu.20272
64. Lara-Ramírez R, Zieger E, Schubert M (2013) Retinoic acid signaling in spinal cord development. Int J Biochem Cell Biol 45:1302–1313. doi: 10.1016/j.biocel.2013.04.002
65. Cornide-Petronio ME, Anadón R, Barreiro-Iglesias A, Rodicio MC (2015) Tryptophan hydroxylase and serotonin receptor 1A expression in the retina of the sea lamprey. Exp Eye Res 135:81–87. doi: 10.1016/j.exer.2015.04.017
66. Goldstein DS, Holmes C (2008) Neuronal Source of Plasma Dopamine. Clin Chem 54:1864–1871. doi: 10.1373/clinchem.2008.107193
67. Rubí B, Maechler P (2010) Minireview: new roles for peripheral dopamine on metabolic control and tumor growth: let's seek the balance. Endocrinology 151:5570–5581. doi: 10.1210/en.2010-0745
68. Misu Y, Kitahama K, Goshima Y (2003) L-3, 4-Dihydroxyphenylalanine as a neurotransmitter candidate in the central nervous system. Pharmacol Ther 97:117–137.
69. Hiroshima Y, Miyamoto H, Nakamura F, et al (2014) The protein Ocular albinism 1 is the orphan GPCR GPR143 and mediates depressor and bradycardic responses to DOPA in the nucleus tractus solitarii. Br J Pharmacol 171:403–414. doi: 10.1111/bph.12459
70. Lopez VM, Decatur CL, Stamer WD, et al (2008) L-DOPA is an endogenous ligand for OA1. PLoS Biol 6:e236. doi: 10.1371/journal.pbio.0060236
71. Fedorow H, Tribl F, Halliday G, et al (2005) Neuromelanin in human dopamine neurons: comparison with peripheral melanins and relevance to Parkinson's disease. Prog Neurobiol 75:109–124. doi: 10.1016/j.pneurobio.2005.02.001
72. Tang H (2009) Regulation and function of the melanization reaction in *Drosophila*. Fly (Austin) 3:105–111. doi: 10.4161/fly.3.1.7747
73. Solano F (2014) Melanins: skin pigments and much more—types, structural models, biological functions, and formation routes. New J Sci 2014:1–28. doi: 10.1155/2014/498276
74. Moret F, Christiaen L, Deyts C, et al (2005) The dopamine-synthesizing cells in the

swimming larva of the tunicate *Ciona intestinalis* are located only in the hypothalamus-related domain of the sensory vesicle. Eur J Neurosci 21:3043–3055. doi: 10.1111/j.1460-9568.2005.04147.x
75. Zega G, Pennati R, Groppelli S, et al (2005) Dopamine and serotonin modulate the onset of metamorphosis in the ascidian *Phallusia mammillata*. Dev Biol 282:246–256. doi: 10.1016/j.ydbio.2005.03.012
76. Jeong H, Kim M-S, Kim S-W, et al (2006) Regulation of tyrosine hydroxylase gene expression by retinoic acid receptor. J Neurochem 98:386–394. doi: 10.1111/j.1471-4159.2006.03866.x
77. Zieger E, Schubert M (2017) New insights into the roles of retinoic acid signaling in nervous system development and the establishment of neurotransmitter systems. In: Int. Rev. Cell Mol. Biol. Elsevier, pp 1–84
78. Chatzi C, Scott RH, Pu J, et al (2009) Derivation of homogeneous GABAergic neurons from mouse embryonic stem cells. Exp Neurol 217:407–416. doi: 10.1016/j.expneurol.2009.03.032
79. Shan Z-Y, Liu F, Lei L, et al (2011) Generation of dorsal spinal cord GABAergic neurons from mouse embryonic stem cells. Cell Reprogramming 13:85–91. doi: 10.1089/cell.2010.0055
80. Addae C, Yi X, Gernapudi R, et al (2012) All-*trans*-retinoid acid induces the differentiation of encapsulated mouse embryonic stem cells into GABAergic neurons. Differentiation 83:233–241. doi: 10.1016/j.diff.2012.03.001
81. Kim J-I, Ganesan S, Luo SX, et al (2015) Aldehyde dehydrogenase 1a1 mediates a GABA synthesis pathway in midbrain dopaminergic neurons. Science 350:102–106. doi: 10.1126/science.aac4690
82. Clagett-Dame M, McNeill EM, Muley PD (2006) Role of all-*trans* retinoic acid in neurite outgrowth and axonal elongation. J Neurobiol 66:739–756. doi: 10.1002/neu.20241
83. Lemons D, McGinnis W (2006) Genomic evolution of *Hox* gene clusters. Science 313:1918–1922. doi: 10.1126/science.1132040
84. Ferrier DE, Minguillón C, Holland PW, Garcia-Fernàndez J (2000) The amphioxus *Hox* cluster: deuterostome posterior flexibility and *Hox14*. Evol Dev 2:284–293.
85. Schubert M (2004) Retinoic acid signaling acts via *Hox1* to establish the posterior limit of the pharynx in the chordate amphioxus. Development 132:61–73. doi: 10.1242/dev.01554
86. Koop D, Chen J, Theodosiou M, et al (2014) Roles of retinoic acid and *Tbx1/10* in pharyngeal segmentation: amphioxus and the ancestral chordate condition. EvoDevo 5:36. doi: 10.1186/2041-9139-5-36
87. Cunningham TJ, Duester G (2015) Mechanisms of retinoic acid signalling and its roles in organ and limb development. Nat Rev Mol Cell Biol 16:110–123. doi: 10.1038/nrm3932
88. Duester G (2008) Retinoic acid synthesis and signaling during early organogenesis. Cell 134:921–931. doi: 10.1016/j.cell.2008.09.002
89. Castelli-Gair Hombría J, Sánchez-Higueras C, Sánchez-Herrero E (2016) Control of organogenesis by *Hox* genes. In: Castelli-Gair Hombría J, Bovolenta P (eds) Organog. Gene Netw. Springer International Publishing, Cham, pp 319–373
90. Parker HJ, Bronner ME, Krumlauf R (2016) The vertebrate *Hox* gene regulatory network for hindbrain segmentation: evolution and diversification. BioEssays 38:526–538. doi: 10.1002/bies.201600010
91. Parker HJ, Bronner ME, Krumlauf R (2014) A *Hox* regulatory network of hindbrain segmentation is conserved to the base of vertebrates. Nature 514:490–493. doi: 10.1038/nature13723
92. Philippidou P, Dasen JS (2013) *Hox* genes: choreographers in neural development,

architects of circuit organization. Neuron 80:12–34. doi: 10.1016/j.neuron.2013.09.020
93. Sheth R, Bastida MF, Kmita M, Ros M (2014) "Self-regulation," a new facet of *Hox* genes' function: *Hox* gene regulation during limb development. Dev Dyn 243:182–191. doi: 10.1002/dvdy.24019
94. Lonfat N, Duboule D (2015) Structure, function and evolution of topologically associating domains (TADs) at *HOX* loci. FEBS Lett 589:2869–2876. doi: 10.1016/j.febslet.2015.04.024
95. Bel-Vialar S, Itasaki N, Krumlauf R (2002) Initiating *Hox* gene expression: in the early chick neural tube differential sensitivity to FGF and RA signaling subdivides the *HoxB* genes in two distinct groups. Development 129:5103–5115.
96. Acemel RD, Tena JJ, Irastorza-Azcarate I, et al (2016) A single three-dimensional chromatin compartment in amphioxus indicates a stepwise evolution of vertebrate *Hox* bimodal regulation. Nat Genet. doi: 10.1038/ng.3497
97. Wada H, Escriva H, Zhang S, Laudet V (2006) Conserved RARE localization in amphioxus *Hox* clusters and implications for *Hox* code evolution in the vertebrate neural crest. Dev Dyn 235:1522–1531. doi: 10.1002/dvdy.20730
98. Bertrand S, Aldea D, Oulion S, et al (2015) Evolution of the role of RA and FGF signals in the control of somitogenesis in chordates. PLOS ONE 10:e0136587. doi: 10.1371/journal.pone.0136587
99. Bertrand S, Camasses A, Somorjai I, et al (2011) Amphioxus FGF signaling predicts the acquisition of vertebrate morphological traits. Proc Natl Acad Sci 108:9160–9165. doi: 10.1073/pnas.1014235108
100. Natale A, Sims C, Chiusano ML, et al (2011) Evolution of anterior *Hox* regulatory elements among chordates. BMC Evol Biol 11:330. doi: 10.1186/1471-2148-11-330
101. Carta M, Stancampiano R, Tronci E, et al (2006) Vitamin A deficiency induces motor impairments and striatal cholinergic dysfunction in rats. Neuroscience 139:1163–1172. doi: 10.1016/j.neuroscience.2006.01.027
102. Romand R, Krezel W, Beraneck M, et al (2013) Retinoic acid deficiency impairs the vestibular function. J Neurosci 33:5856–5866. doi: 10.1523/JNEUROSCI.4618-12.2013
103. Srour M, Caron V, Pearson T, et al (2016) Gain-of-function mutations in *RARB* cause intellectual disability with progressive motor impairment: HUMAN MUTATION. Hum Mutat 37:786–793. doi: 10.1002/humu.23004
104. Wang Y, Chen J, Du C, et al (2014) Characterization of retinoic acid-induced neurobehavioral effects in developing zebrafish. Environ Toxicol Chem 33:431–437. doi: 10.1002/etc.2453
105. Krezel W, Ghyselinck N, Samad TA, et al (1998) Impaired locomotion and dopamine signaling in retinoid receptor mutant mice. Science 279:863–867.
106. Samad TA, Krezel W, Chambon P, Borrelli E (1997) Regulation of dopaminergic pathways by retinoids: activation of the D2 receptor promoter by members of the retinoic acid receptor–retinoid X receptor family. Proc Natl Acad Sci 94:14349–14354.
107. Wong LS, Eshel G, Dreher J, et al (1991) Role of dopamine and GABA in the control of motor activity elicited from the rat nucleus accumbens. Pharmacol Biochem Behav 38:829–835.
108. Watanabe M, Maemura K, Kanbara K, et al (2002) GABA and GABA receptors in the central nervous system and other organs. In: Int. Rev. Cytol. Elsevier, pp 1–47
109. Draper A, Stephenson MC, Jackson GM, et al (2014) Increased GABA Contributes to Enhanced Control over Motor Excitability in Tourette Syndrome. Curr Biol 24:2343–2347. doi: 10.1016/j.cub.2014.08.038
110. Fink AJP, Croce KR, Huang ZJ, et al (2014) Presynaptic inhibition of spinal sensory feedback ensures smooth movement. Nature 509:43–48. doi: 10.1038/nature13276

111. Windhorst U (2007) Muscle proprioceptive feedback and spinal networks. Brain Res Bull 73:155–202. doi: 10.1016/j.brainresbull.2007.03.010
112. Brown ER, Nishino A, Bone Q, et al (2005) GABAergic synaptic transmission modulates swimming in the ascidian larva. Eur J Neurosci 22:2541–2548. doi: 10.1111/j.1460-9568.2005.04420.x
113. Mikhaleva Y, Kreneisz O, Olsen LC, et al (2015) Modification of the larval swimming behavior in *Oikopleura dioica*, a chordate with a miniaturized central nervous system by dsRNA injection into fertilized eggs. J Exp Zoolog B Mol Dev Evol 324:114–127. doi: 10.1002/jez.b.22607
114. Nakayama K, Nishimaru H, Kudo N (2002) Basis of changes in left–right coordination of rhythmic motor activity during development in the rat spinal cord. J Neurosci 22:10388–10398.
115. Johnston GA (2013) Advantages of an antagonist: bicuculline and other GABA antagonists. Br J Pharmacol 169:328–336. doi: 10.1111/bph.12127
116. Garcia P, Kolesky S, Jenkins A (2010) General anesthetic actions on GABAA receptors. Curr Neuropharmacol 8:2–9. doi: 10.2174/157015910790909502
117. Rudolph U, Möhler H (2004) Analysis of GABAA receptor function and dissection of the pharmacology of benzodiazepines and general anesthetics through mouse genetics. Annu Rev Pharmacol Toxicol 44:475–498. doi: 10.1146/annurev.pharmtox.44.101802.121429
118. Trudell JR, Messing RO, Mayfield J, Harris RA (2014) Alcohol dependence: molecular and behavioral evidence. Trends Pharmacol Sci 35:317–323. doi: 10.1016/j.tips.2014.04.009
119. Fuentes M, Schubert M, Dalfo D, et al (2004) Preliminary observations on the spawning conditions of the European amphioxus (*Branchiostoma lanceolatum*) in captivity. J Exp Zoolog B Mol Dev Evol 302:384–391. doi: 10.1002/jez.b.20025
120. Fuentes M, Benito E, Bertrand S, et al (2007) Insights into spawning behavior and development of the European amphioxus *Branchiostoma lanceolatum*. J Exp Zoolog B Mol Dev Evol 308:484–493. doi: 10.1002/jez.b.21179
121. Theodosiou M, Colin A, Schulz J, et al (2011) Amphioxus spawning behavior in an artificial seawater facility. J Exp Zoolog B Mol Dev Evol 316:263–275. doi: 10.1002/jez.b.21397
122. Holland LZ, Yu J-K (2004) Cephalochordate (amphioxus) embryos: procurement, culture, and basic methods. Methods Cell Biol 74:195–215.
123. Schneider CA, Rasband WS, Eliceiri KW (2012) NIH Image to ImageJ: 25 years of image analysis. Nat Methods 9:671–675.
124. Oulion S, Bertrand S, Belgacem MR, et al (2012) Sequencing and analysis of the Mediterranean amphioxus (*Branchiostoma lanceolatum*) transcriptome. PloS One 7:e36554. doi: 10.1371/journal.pone.0036554
125. Edgar RC (2004) MUSCLE: multiple sequence alignment with high accuracy and high throughput. Nucleic Acids Res 32:1792–1797. doi: 10.1093/nar/gkh340
126. Capella-Gutierrez S, Silla-Martinez JM, Gabaldon T (2009) trimAl: a tool for automated alignment trimming in large-scale phylogenetic analyses. Bioinformatics 25:1972–1973. doi: 10.1093/bioinformatics/btp348
127. Stamatakis A, Hoover P, Rougemont J (2008) A rapid bootstrap algorithm for the RAxML web servers. Syst Biol 57:758–771. doi: 10.1080/10635150802429642
128. Darriba D, Taboada GL, Doallo R, Posada D (2011) ProtTest 3: fast selection of best-fit models of protein evolution. Bioinformatics 27:1164–1165. doi: 10.1093/bioinformatics/btr088
129. Yu JKS, Holland LZ (2009) Extraction of RNA from amphioxus embryos or adult amphioxus tissue. Cold Spring Harb Protoc 2009:pdb.prot5288. doi: 10.1101/pdb.prot5288

130. Pascual-Anaya J, D'Aniello S, Garcia-Fernàndez J (2008) Unexpectedly large number of conserved noncoding regions within the ancestral chordate *Hox* cluster. Dev Genes Evol 218:591–597. doi: 10.1007/s00427-008-0246-8
131. Yu JKS, Holland LZ (2009) Amphioxus whole-mount in *situ* hybridization. Cold Spring Harb Protoc 2009:pdb.prot5286. doi: 10.1101/pdb.prot5286
132. Candiani S, Lacalli TC, Parodi M, et al (2008) The cholinergic gene locus in amphioxus: molecular characterization and developmental expression patterns. Dev Dyn 237:1399–1411. doi: 10.1002/dvdy.21541

Figure captions

Fig.1 Effects of altered retinoic acid (RA) signaling levels on the development of serotonergic cells in amphioxus. Animals were stained with an antibody against serotonin (5-HT) (green), an antibody against acetylated tubulin (AT) (red), and the nucleic acid dye Hoechst (blue). The images show lateral views with the rostral end directed towards the right. (a-d) Normal development of 5-HT neurons in amphioxus larvae at different developmental stages from 36 to 108 hpf (hours post fertilization). (a'-d') Close-ups featuring the heads of the amphioxus larvae shown in (a-d), respectively. (c'') Bright-field image of the cerebral vesicle of an amphioxus larva at 60 hpf showing the pigment spot of the frontal eye (black) and 5-HT immunoreactivity (green). (e-g,f',g') 5-HT immunoreactive neurons in amphioxus larvae at 60 hpf that were treated with DMSO (Control) (e), with the RA receptor (RAR) antagonist BMS493 (f,g) or with all-*trans* RA (f',g') at different developmental time points (t:), at 6 or 24 hpf. Abbreviations: cv – cerebral vesicle, np – neuropore, ps – pigment spot, rn – rostral nerves. Scale bar in (a) also applies to (b-d), scale bar in (a') also applies to (b'-d'), and scale bar in (e) applies also to (f,g,f',g').

Fig.2 Effects of altered retinoic acid (RA) signaling levels on the development of dopaminergic cells in amphioxus. All animals were stained with an antibody against dopamine (DA) (green), an antibody against acetylated tubulin (AT) (red), and the nucleic acid dye Hoechst (blue). (a-d) Normal development of DA immunoreactive (-ir) cells in amphioxus larvae at different developmental stages, from 36 to 108 hpf (hours post fertilization). Lateral views with rostral ends directed towards the upper right corner of the images. (a'-d') Close-ups featuring heads of the amphioxus larvae shown in (a-d), respectively. (c'') Close-up of the DA-ir cell cluster of the amphioxus larva shown in (c,c'). The arrowhead indicates an array of small AT-ir structures that are typically associated with the DA-ir cell cluster of the right papilla. (e) Dorsal view of the head of an amphioxus larva at 60 hpf, showing the position of the DA-ir cell cluster on the right side of the animal. (f) Average number and standard deviation (σ) of DA-ir cells in amphioxus larvae at 60 hpf that were treated with DMSO (Control, green bar), with the RA receptor (RAR) antagonist BMS493 (blue bars) or with all-*trans* RA (red bars) at different developmental time points (t:), as indicated below the x-axis. The number (n) of animals counted for each condition is given at the base of

each colored bar. An asterisk (*) above an error bar indicates that the difference between this condition and the control is statistically significant. (g-l,h'-l') DA-ir cells in amphioxus larvae at 60 hpf that were treated with DMSO (Control) (g), with the RAR antagonist BMS493 (h-l) or with all-*trans* RA (h'-l') at different developmental time points (t:), between 6 and 48 hpf. Brackets indicate the size and anterior-posterior expansion of the DA-ir cell cluster. Abbreviations: dac – DA-ir cell cluster of the right papilla, es – endostyle, gs – gill slit, m – mouth, np – neuropore, pop – pre-oral pit. Scale bar in (a) also applies to (b-e), scale bar in (a') also applies to (b'-d'), and scale bar in (g) also applies to (h-l,h'-l').

Fig.3 Effects of altered retinoic acid (RA) signaling levels on the development of tyrosine hydroxylase (TH) immunoreactive (-ir) cells in amphioxus. All animals were stained with an antibody against TH (green), an antibody against acetylated tubulin (AT) (red), and the nucleic acid dye Hoechst (blue). Lateral views with rostral ends directed towards the right. (a-d) Normal development of TH-ir cells in amphioxus larvae at different developmental stages from 36 to 108 hpf (hours post fertilization). (a'-c') Close-ups featuring heads of the amphioxus larvae shown in (a-c), respectively. Arrows in (c') indicate two clusters of small TH-ir cells within the endostyle. (c'') Close-up of the TH-ir cell cluster of the amphioxus larvae shown in (c,c'). The arrowhead indicates the array of AT-ir structures that is typically associated with the TH/DA-ir cell cluster of the right papilla. (e-g) TH-ir cells in the head of amphioxus larvae at 60 hpf that were treated with DMSO (Control) (e), with the RA receptor (RAR) antagonist BMS493 (f) or with all-*trans* RA (g) at 6 hpf (t:6). White boxes highlight the position of the TH-ir cell cluster of the right papilla. (e'-g') Close-ups of boxed areas in (e-g), respectively. Arrowheads indicate the array of AT-ir structures that is typically associated with the TH/DA-ir cell cluster of the right papilla. Abbreviations: csg – club-shaped gland, cth – cerebral TH-ir cells, dac – TH-ir cell cluster corresponding to the DA-ir cell cluster of the right papilla, es – endostyle, gs – gill slit, np –neuropore, ps – pigment spot. Scale bar in (a) also applies to (b-d), scale bar in (a') also applies to (b',c'), scale bar in (e) also applies to (f,g), and scale bar in (e') also applies to (f',g').

Fig.4 Normal development of GABA immunoreactive (-ir) cells in amphioxus. All animals were stained with an antibody against GABA (green), an antibody against acetylated tubulin (AT) (red), and the nucleic acid dye Hoechst (blue). (a-f) Lateral views of amphioxus embryos and larvae at different developmental stages, from 24 to 108 hpf (hours post fertilization). Heads are directed towards the right. Arrowheads in (d) indicate weakly stained GABAergic neurons in the mid-region of the neural tube. (c1-c4) Close-ups of the numbered GABA-ir structures in (c). Arrowheads in (c4) point at putative axonal growth cones. (g,g',g'') Close-ups of the head (g), oral region (g'), and lateral ectoderm (g'') of an amphioxus larva at 60 hpf. Arrows indicate GABA-ir epidermal sensory neurons (ESNs). (g') Arrowheads pointing upward indicate GABA-ir neurons of the oral plexus that form a ring around the mouth. The arrowhead pointing downward indicates the anterior-most GABA-ir neuron of the oral plexus, which is located at the pre-oral pit and innervates both the mouth and first gill slit. Scale bar in (a) also applies to (b-f) and scale bar in (c1) also applies to (c2-c4).

Fig.5 Effects of altered retinoic acid (RA) signaling levels on the development of GABA immunoreactive (-ir) cells in the amphioxus central nervous system (CNS). All images show lateral views of amphioxus larvae at 36 hpf (hours post fertilization) with their rostral end directed towards the right. The animal in (a) was stained with an antibody against GABA (green), an antibody against acetylated tubulin (AT) (red), and the nucleic acid dye Hoechst (blue). In (b-d,a'-d'), the fluorescent signal for GABA-ir (black) has been color-inverted to provide a better contrast. (a,a') Control animal treated at 6 hpf with DMSO. (b-d) Animals treated with the RA receptor (RAR) antagonist BMS493 at different developmental time points (t:), between 6 and 24 hpf. (b'-d') Animals treated with all-*trans* RA at different developmental time points. Scale bar in (a) applies to all images. (e) For amphioxus larvae at 36 hpf treated with the indicated conditions, the average number of GABA-ir cell clusters in the neural tube is depicted by colored bars and the standard deviation (σ) by error bars. Controls are in green, BMS493-treated animals in blue, and RA-treated animals in red. The time point of treatment (between 6 and 24 hpf) is given below the x-axis. The number (n) of animals counted for each condition is indicated at the base of each colored bar. An

asterisk (*) above an error bar indicates that the difference between this condition and the control is statistically significant.

Fig.6 Effects of altered retinoic acid (RA) signaling levels on the development of GABA immunoreactive (-ir) cells in the amphioxus peripheral nervous system (PNS). All images show lateral views of amphioxus larvae at 60 hpf (hours post fertilization) with their rostral end directed towards the right. The animal in (a) was stained with an antibody against GABA (green), an antibody against acetylated tubulin (AT) (red), and the nucleic acid dye Hoechst (blue). In (b-d,a'-d') the fluorescent signal for GABA (black) has been color-inverted to provide a better contrast. (a,a') Control animal treated at 6 hpf with DMSO. (b-d) Animals treated with the RA receptor (RAR) antagonist BMS493 at different developmental time points (t:), between 6 and 24 hpf. (b'-d') Animals treated with all-*trans* RA at different developmental time points. Scale bar in (a) applies to all images. (e) For amphioxus larvae at 60 hpf treated with the indicated conditions, the average number of GABA-ir epidermal sensory neurons (ESNs) is depicted by colored bars and the standard deviation (σ) by error bars. Controls are in green, BMS493-treated animals in blue, and RA-treated animals in red. Treatment time points, between 6 and 24 hpf, are given in the upper right corner of each diagram. The number (n) of animals counted for each condition is indicated at the base of the colored bars. An asterisk (*) above an error bar indicates that the difference between this condition and the control is statistically significant. The image below the first diagram shows the color-inverted fluorescent signal for the nucleic acid dye Hoechst in an amphioxus larva at 60 hpf. The dotted lines provide an indication of the three ectodermal sections, in which GABA-ir ESNs were counted (Anterior, Middle, and Posterior).

Fig.7 Correlation between the effects of retinoic acid (RA) signaling on *Hox* gene expression and the formation of specific neural cell populations in amphioxus larvae. The animals are shown in lateral (a-o) or dorsal views (a'-c',g'-l'). (a-f,a'-c') Correlation between RA dependency of *Hox1* expression and dopamine (DA) immunoreactive (-ir) cells in the ectoderm of amphioxus larvae at 36 hpf (hours post

fertilization). (a-c,a'-c') *Hox1* expression in larvae treated at 6 hpf with either DMSO (a,a'), the RA receptor (RAR) antagonist BMS493 (b,b') or all-*trans* RA (c,c'). Arrowheads highlight anterior expression limits of *Hox1* in the ectoderm. (d-f) DA-ir (green) as well as acetylated tubulin (AT)-ir (red), and Hoechst nucleic acid staining (blue) in amphioxus larvae that were treated at 6 hpf with either DMSO (d), BMS493 (e) or all-*trans* RA (f). Brackets mark expansion of the DA-ir cell cluster. (g-o,g'-l') Correlation between RA dependency of *Hox3* expression and *GAD*-expressing cell clusters (numbered from anterior to posterior) in the central nervous system (CNS) of amphioxus larvae at 30 hpf. (g-i,g'-i') *Hox3* expression in amphioxus larvae treated at 6 hpf with either DMSO (g,g'), BMS493 (h,h') or all-*trans* RA (i,i'). Arrowheads indicate anterior expression limits of *Hox3* in the CNS. (j-l,j'-l') *GAD*-expressing cells in amphioxus larvae treated at 6 hpf with either DMSO (j,j'), BMS493 (k,k') or all-*trans* RA (l,l'). (m-o) Co-localization of *Hox3* expression (yellow) and *GAD*-expressing cells (red), numbered from anterior to posterior, in amphioxus larvae that were treated at 6 hpf with either DMSO (m), BMS493 (n) or all-*trans* RA (o). Scale bar in (a) also applies to (b-f,a'-c') and scale bar in (g) also applies to (h-o,g'-l').

Fig.8 Effects of retinoic acid (RA) signaling on the muscular swimming motion of amphioxus larvae. Larvae were treated at specific time points (t:), 6 or 24 hpf (hours post fertilization), with either DMSO (Control), the RA receptor (RAR) antagonist BMS493 or all-*trans* RA and assayed at 60 hpf. During muscular swimming, the changing body outline of the larvae is depicted at 10 msec intervals. For each condition, a representative larva was chosen to show how the maximum inner curvature (MIC) was measured, by fitting a circle (red) into the most curved portion of the larval body. The average MIC of ten amphioxus larvae is given on the right, with the standard deviation (σ) indicated in brackets.

Fig.9 Model of the retinoic acid (RA) signaling-dependent establishment of specific neural cell populations in early amphioxus larva. (a) Formation of an ectodermal cell cluster comprising dopamine (DA) immunoreactive cells. (b) Formation of three GABA immunoreactive cell clusters in the central nervous system (CNS). RA is

synthesized in the posterior portion of the larva (orange) and diffuses anteriorly, where specific enzymes of the CYP26 family ensure local RA degradation (green). RA signaling determines the anterior limits of *Hox1* and *Hox3* expression, with HOX1 and HOX3 (purple), respectively, restricting the formation of dopamine cells in the ectoderm (blue) and of GABA neurons in the CNS (yellow) to the anterior region of the larva. Accordingly, RA signaling demarcates the development of different neural cell populations in amphioxus by modulating the expression of specific *Hox* genes serving distinct functions.

Fig.A1 Effects of altered retinoic acid (RA) signaling levels on the development of visceral GABA immunoreactive (-ir) cells in the amphioxus oral plexus. Close-ups of the heads of amphioxus larvae at 60 hpf (hours post fertilization) with their rostral end directed towards the right. The fluorescent signal for GABA-ir (black) has been color-inverted to provide a better contrast. (a) Control animal treated at 6 hpf with DMSO. (b-d) Animals treated with the RA receptor (RAR) antagonist BMS493 at different developmental time points (t:), between 6 and 24 hpf. The dotted ellipse in (b) highlights supernumerary GABA-ir cells located ventral to the mouth. (b'-d') Animals treated with all-*trans* RA at different developmental time points. Arrowheads indicate the large GABA-ir neuron located at the pre-oral pit. Arrows indicate posterior projections from GABA-ir neurons of the oral plexus to the first gill slit. Scale bar in (a) applies to all images.

Fig.A2 Effects of altered retinoic acid (RA) signaling levels on the development of *GAD*-expressing cells in amphioxus. Lateral (a-k) and dorsal (a'-k') views with rostral ends directed towards the right. (a-e,a'-e') *GAD* expression during normal development in amphioxus embryos and larvae at different stages, from 24 to 60 hpf (hours post fertilization). (e,e') Close-ups of the head of the amphioxus larva shown in (d,d'). The arrowhead in (a) indicates the first detectable *GAD*-expressing cell in the neural tube of an amphioxus neurula. Arrowheads in (c,c') indicate *GAD* expression in epidermal sensory neurons (ESNs). The arrowhead in (e) indicates *GAD*-expressing cells in the ectoderm around the mouth (oral plexus) of an

amphioxus larva. (f-k,f'-k') *GAD*-expressing cells in amphioxus larvae at 36 (f-h,f'-h') and 60 hpf (i-k,i'-k') treated at 6 hpf (t:6) with DMSO (Control) (f,i,f,',i'), with the RA receptor (RAR) antagonist BMS493 (g,j,g',j') or with all-*trans* RA (h,k,h',k'). *GAD*-expressing cell clusters in the central nervous system (CNS) that correspond to GABA-ir cell clusters (Fig.4) are numbered accordingly. Scale bars in (a-e) respectively also apply to (a'-e'), scale bar in (f) also applies to (g,h,f'-h'), and scale bar in (i) also applies to (j,k,i'-k').

Online Resource 1 Three dimensional (3D) projection of GABA immunoreactive (-ir) cells in the developing amphioxus central nervous system (CNS). 3D projection of amphioxus larva at 36 hpf (hours post fertilization) showing that all three GABA-ir cell clusters in the CNS (white) give rise to neurites that cross the midline (red circles) and project along the contra-lateral side of the neural tube.

Online Resource 2 Effects of retinoic acid (RA) signaling on amphioxus larval motor control. Slow motion videos showing the swimming movements of amphioxus larvae at 48 hpf (hours post fertilization) that were treated as indicated, starting from either 6 hpf (t:6) or 24 hpf (t:24), with either DMSO (Control), the RA receptor (RAR) antagonist BMS493 or all-*trans* retinoic acid (RA).

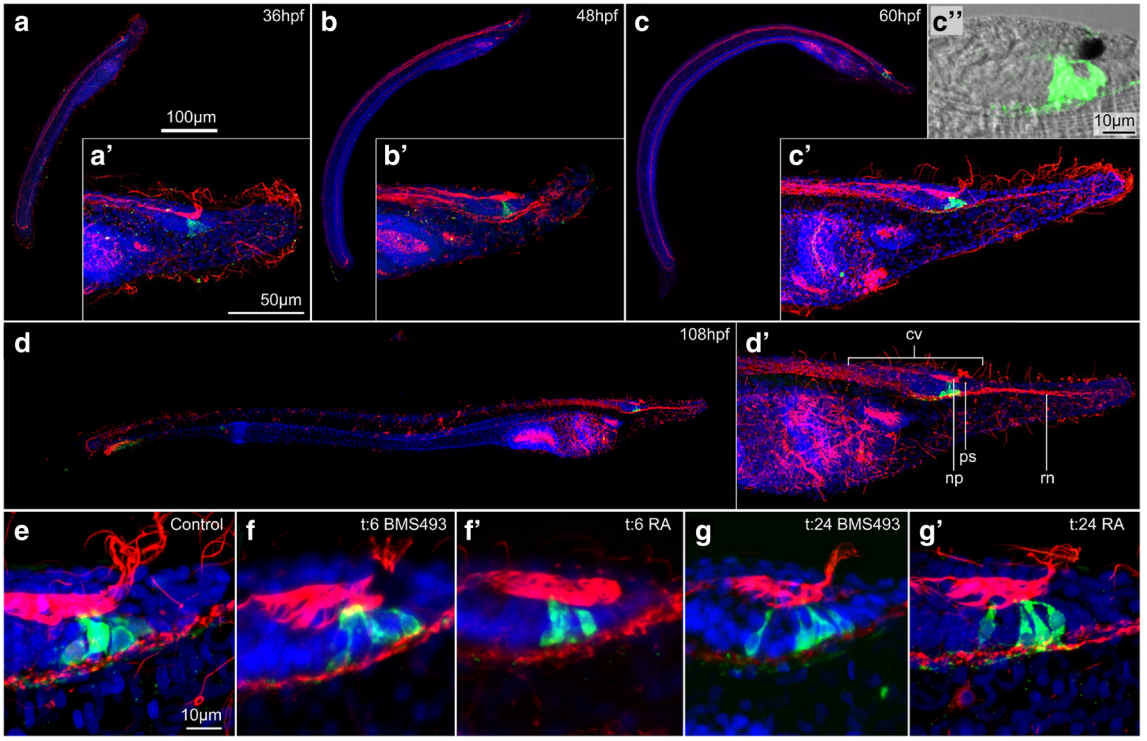
a
36hpf
100µm
a'
50µm
b
48hpf
b'
c
60hpf
c''
10µm
c'
d
108hpf
d'
cv
ps
np
rn
e
Control
10µm
f
t:6 BMS493
f'
t:6 RA
g
t:24 BMS493
g'
t:24 RA

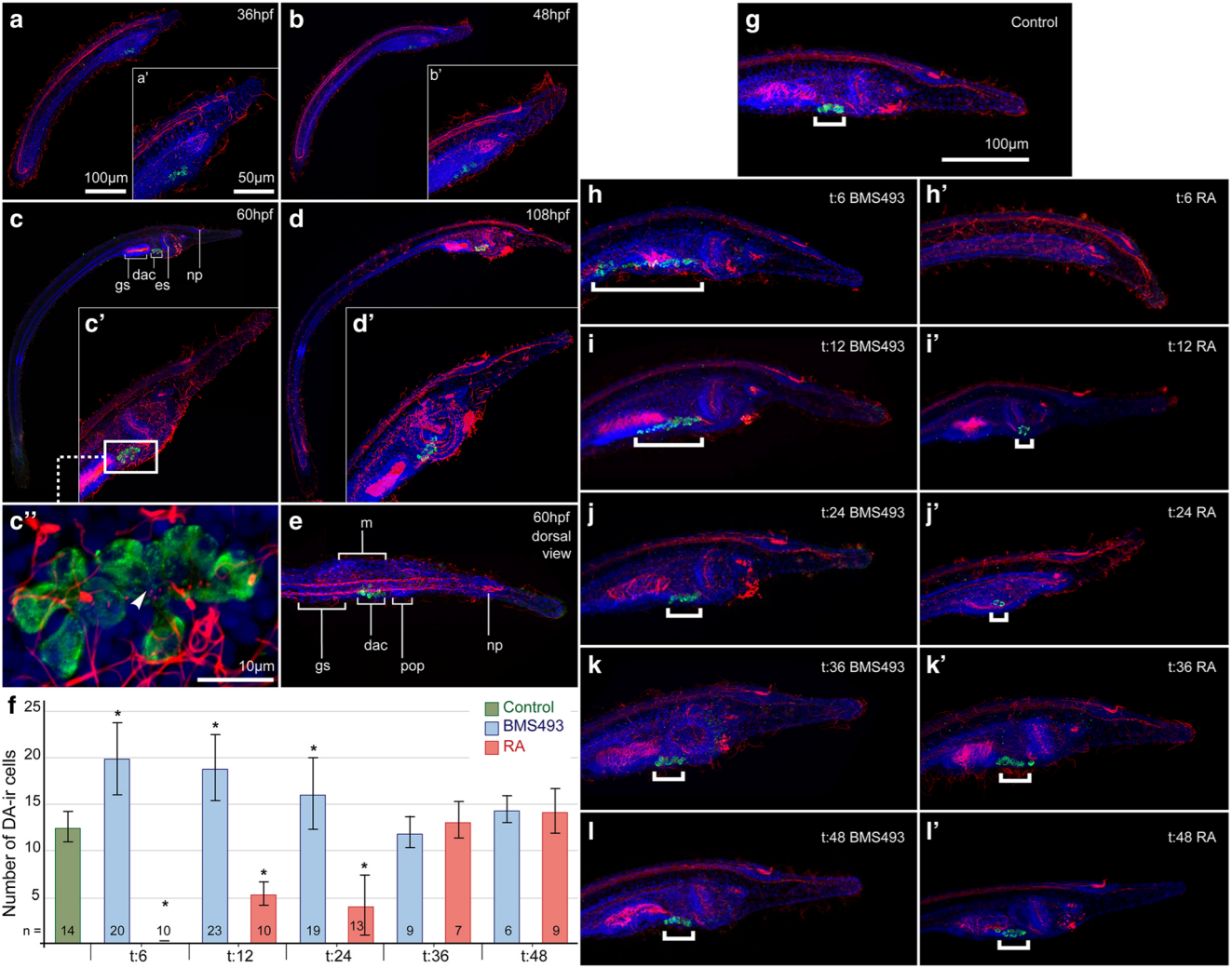
a
36hpf
a'
100µm
50µm
b
48hpf
b'
c
60hpf
gs
dac
es
np
c'
d
108hpf
d'
c''
10µm
e
60hpf
dorsal
view
m
dac
gs
pop
np
f
Control
BMS493
RA
Number of DA-ir cells
n =
14
20
10
23
10
19
13
9
7
6
9
t:6
t:12
t:24
t:36
t:48
g
Control
100µm
h
t:6 BMS493
h'
t:6 RA
i
t:12 BMS493
i'
t:12 RA
j
t:24 BMS493
j'
t:24 RA
k
t:36 BMS493
k'
t:36 RA
l
t:48 BMS493
l'
t:48 RA

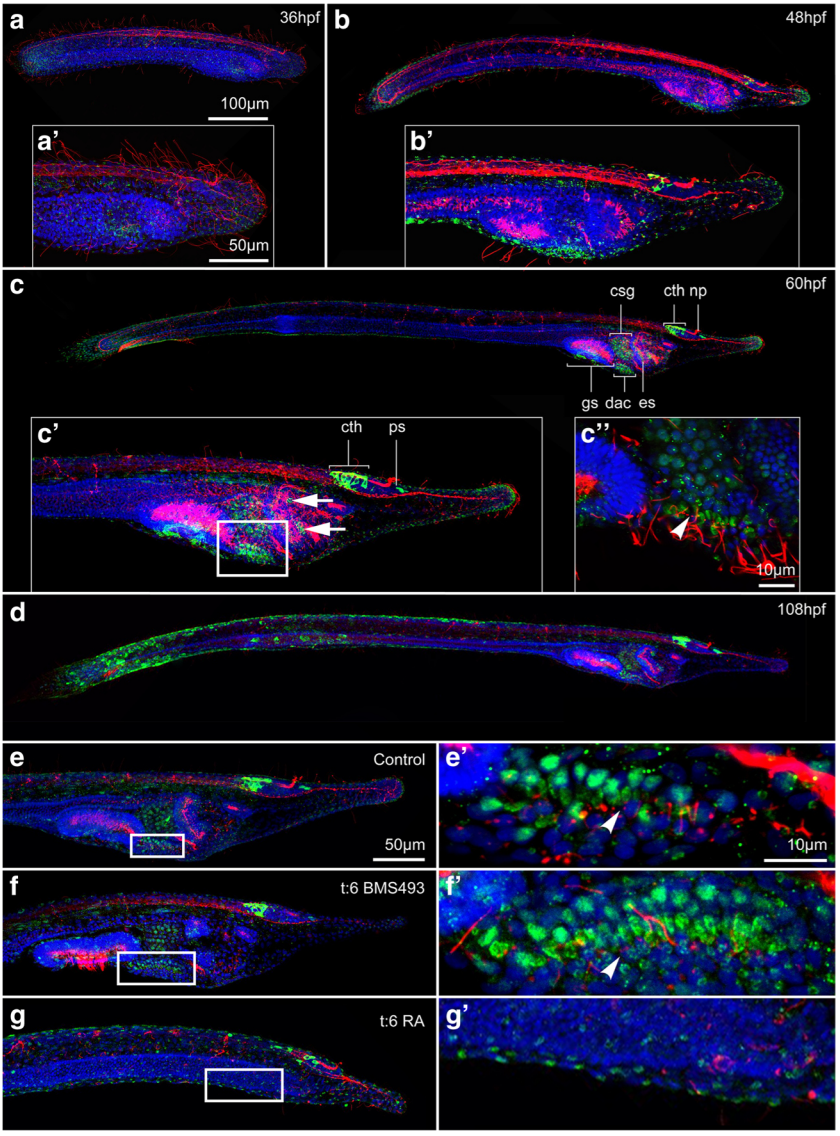
a
36hpf
100µm
a'
50µm
b
48hpf
b'
c
60hpf
csg
cth np
gs dac es
c'
cth
ps
c''
10µm
d
108hpf
e
Control
50µm
e'
10µm
f
t:6 BMS493
f'
g
t:6 RA
g'

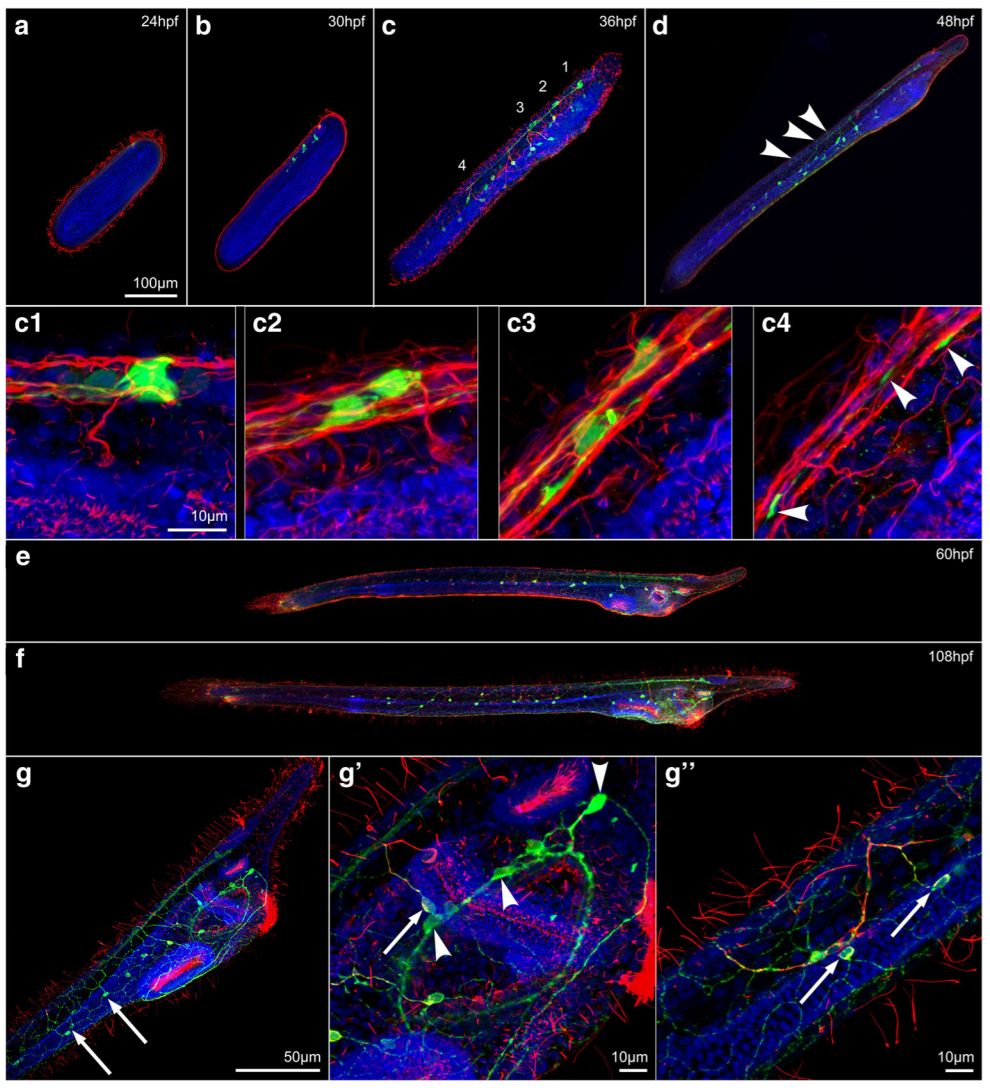
a
24hpf
b
30hpf
c
36hpf
1
2
3
4
d
48hpf
100µm
c1
c2
c3
c4
10µm
e
60hpf
f
108hpf
g
g'
g''
50µm
10µm
10µm

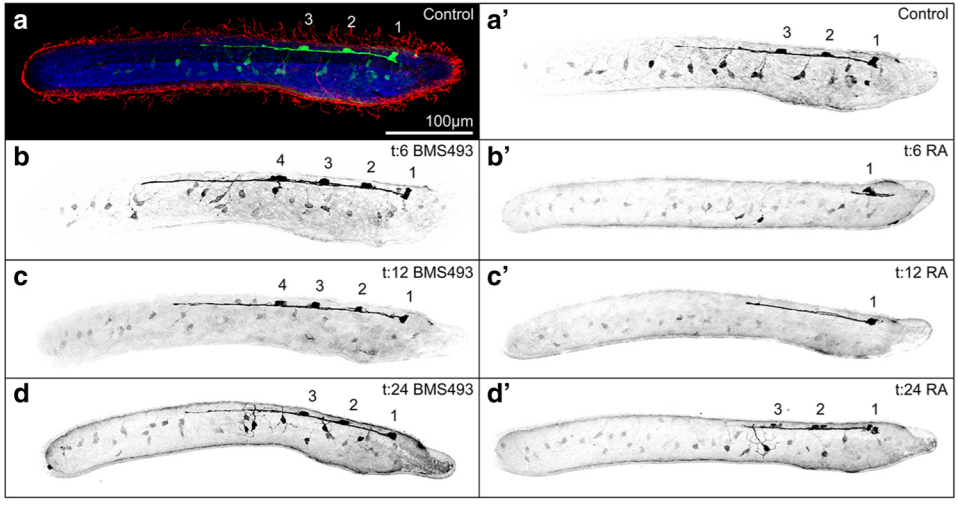
a
Control
3
2
1
100µm
a'
Control
3
2
1
b
t:6 BMS493
4
3
2
1
b'
t:6 RA
1
c
t:12 BMS493
4
3
2
1
c'
t:12 RA
1
d
t:24 BMS493
3
2
1
d'
t:24 RA
3
2
1
e
Number of GABA-ir cell clusters
6
5
4
3
2
1
n=
7
10
10
7
7
9
10
t:6
t:12
t:24
Control
BMS493
RA

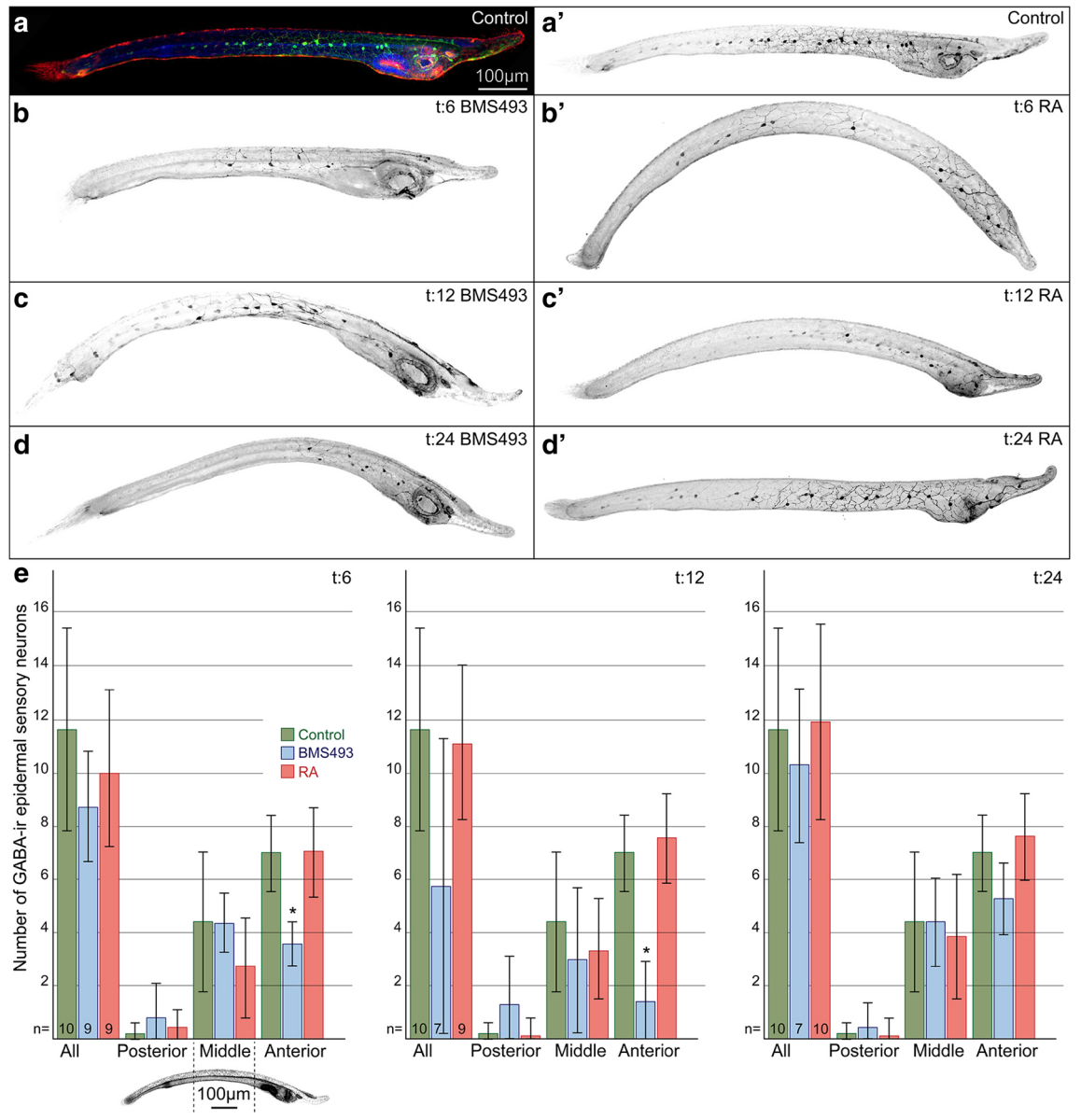
a
Control
100µm
a'
Control
b
t:6 BMS493
b'
t:6 RA
c
t:12 BMS493
c'
t:12 RA
d
t:24 BMS493
d'
t:24 RA
e
t:6
t:12
t:24
Number of GABA-ir epidermal sensory neurons
Control
BMS493
RA
n=
10 9 9
10 7 9
10 7 10
All
Posterior
Middle
Anterior
100µm

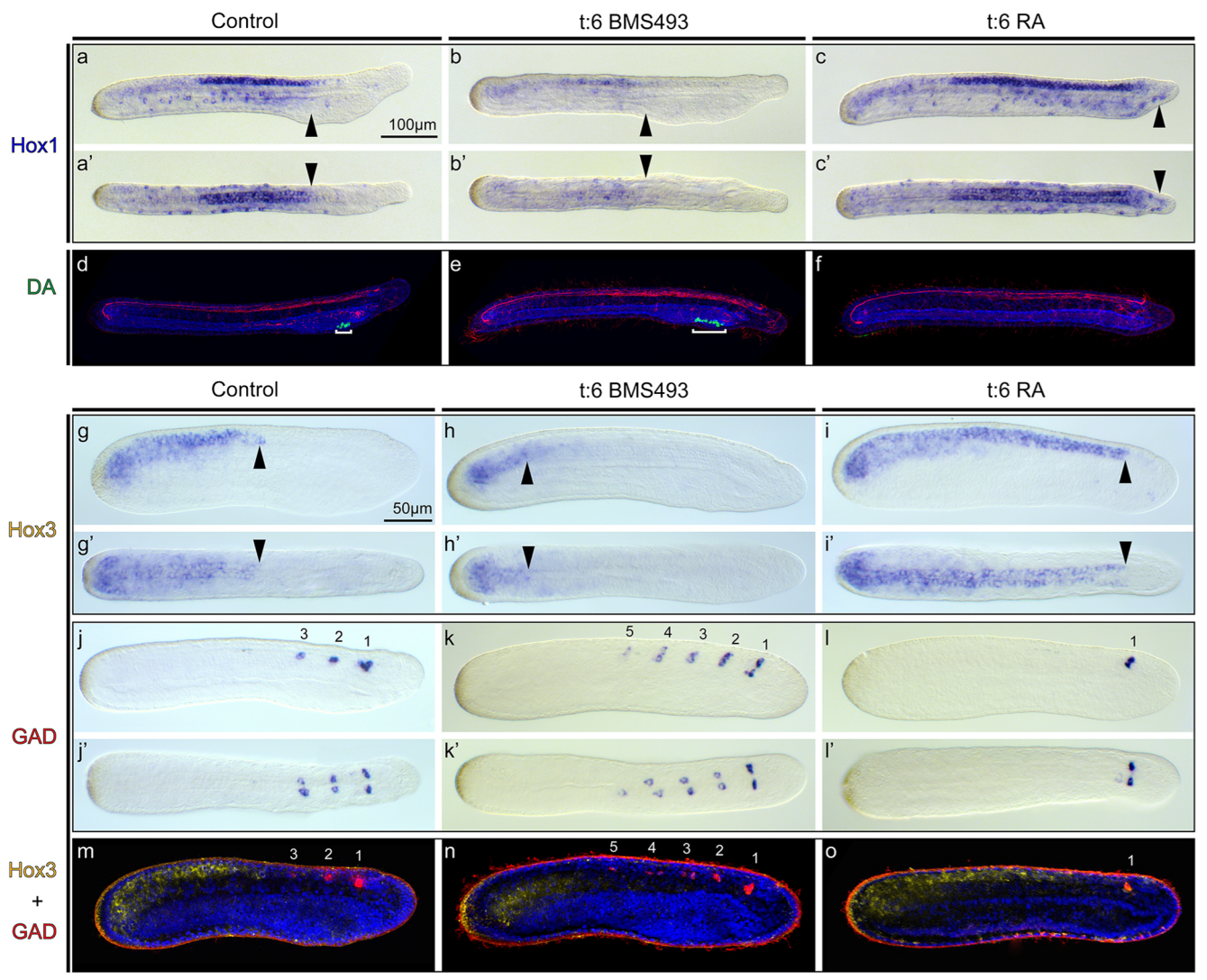
Control
t:6 BMS493
t:6 RA
Hox1
DA
Hox3
GAD
Hox3
+
GAD
a
b
c
a'
b'
c'
d
e
f
g
h
i
g'
h'
i'
j
k
l
j'
k'
l'
m
n
o
100μm
50μm
1
2
3
4
5

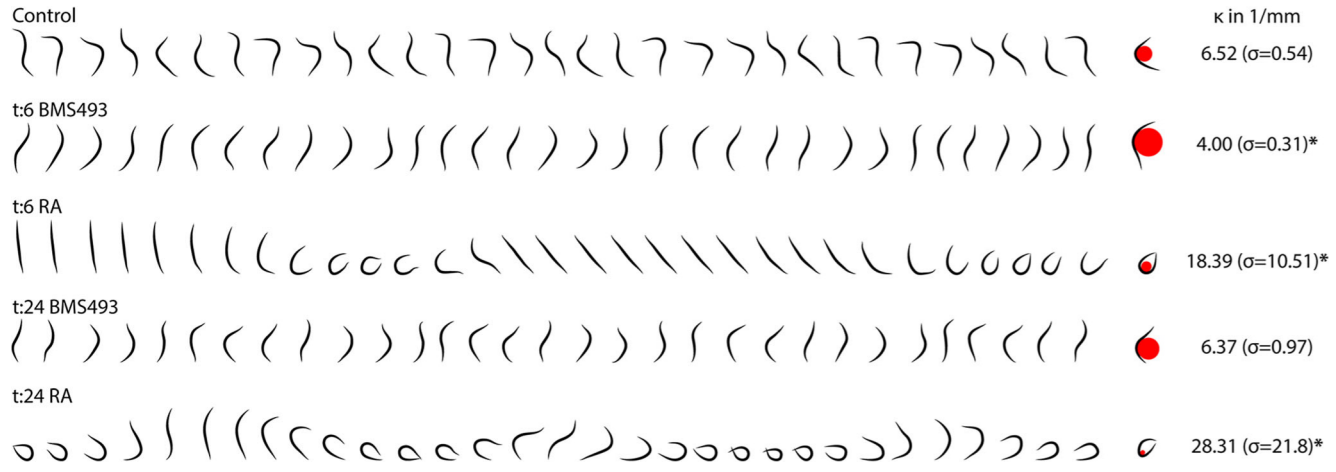
Control
κ in 1/mm
6.52 (σ=0.54)
t:6 BMS493
4.00 (σ=0.31)*
t:6 RA
18.39 (σ=10.51)*
t:24 BMS493
6.37 (σ=0.97)
t:24 RA
28.31 (σ=21.8)*

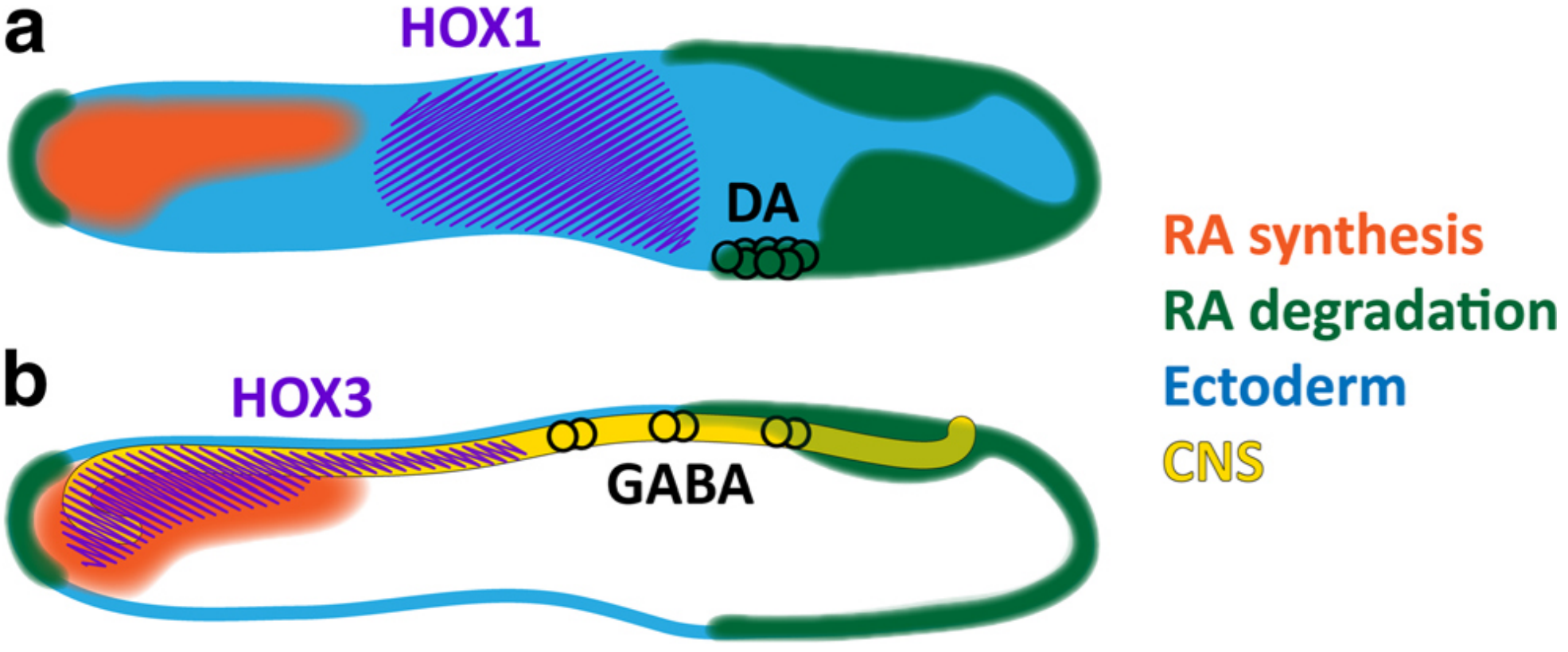
a
HOX1
DA
b
HOX3
GABA
RA synthesis
RA degradation
Ectoderm
CNS